
Article:
Aad, G., Aakvaag, E., Abbott, B. et al. (2026) Search for the Higgs boson decay to a Z boson and a photon in pp collisions at √ s=13 TeV and 13.6 TeV with the ATLAS detector. Physics Letters B, 876. 140313. ISSN: 0370-2693

https://doi.org/10.1016/j.physletb.2026.140313

Phys. Lett. B 876 (2026) 140313

Contents lists available at ScienceDirect

Physics Letters B

journal homepage: www.elsevier.com/locate/physletb

Letter

Search for the Higgs boson decay to a Z boson and a photon in pp collisions at $\sqrt{s} = 13$ TeV and 13.6 TeV with the ATLAS detector

The ATLAS Collaboration [1]

ARTICLE INFO

Editor: Dr. M. Doser

ABSTRACT

A search for the Higgs boson decay to a Z boson and a photon in the $\ell\ell\gamma$ ($\ell = e, \mu$) final state is performed using pp collisions at $\sqrt{s} = 13.6$ TeV recorded with the ATLAS detector at the Large Hadron Collider during 2022–2024, corresponding to an integrated luminosity of 165 fb^{-1}. The signal yield, normalised to the Standard Model prediction, is measured to be $\mu = 0.9^{+0.7}_{-0.6}$, compatible with the expected value of $\mu = 1.0 \pm 0.7$. This corresponds to an observed (expected) signal significance of 1.4 (1.5) standard deviations under the background-only hypothesis. This result is combined with that of a similar search performed with 140 fb^{-1} of $\sqrt{s} = 13$ TeV pp collisions to provide the best expected sensitivity to date to this rare decay, namely an observed (expected) signal strength of $\mu = 1.3^{+0.6}_{-0.5}$ ($\mu = 1.0^{+0.6}_{-0.5}$), corresponding to an observed (expected) significance of 2.5 (1.9) standard deviations. The measurement is consistent with the Standard Model expectation.

1. Introduction

A new boson with properties consistent with those of the Standard Model (SM) Higgs boson (H) was independently observed in 2012 by the ATLAS and CMS Collaborations [1,2] at the Large Hadron Collider (LHC) [3]. Measurements of its couplings to SM particles, its spin, and its parity have, to date, shown no significant deviation from the SM predictions [4–7]. The combined ATLAS and CMS determination of its mass from LHC Run-1 data yields $m_H = 125.09 \pm 0.24$ GeV [8], a value that is consistent with recent Run-2 measurements [9–11].

Within the SM, the Higgs boson decay to a Z boson and a photon ($H \to Z\gamma$) proceeds via loop-induced processes, leading to a predicted branching ratio of $\mathrm{BR}(H \to Z\gamma) = (1.54^{+0.10}_{-0.11}) \times 10^{-3}$ for $m_H = 125.09$ GeV [12], similar to that for $H \to \gamma\gamma$, $\mathrm{BR}(H \to \gamma\gamma) = (2.27^{+0.07}_{-0.06}) \times 10^{-3}$ [12]. The observation of this decay channel, not yet established, would not only complete the suite of established Higgs bosons into pairs of electroweak gauge bosons ($\gamma\gamma$, ZZ^*, WW^*) but also represent a sensitive probe for indirect signs of new physics. In fact, extensions of the SM, such as models with additional colourless charged scalars, fermions, or vector bosons, can alter this rate via contributions in the loops [13–19], making the measurement of $\mathrm{BR}(H \to Z\gamma)$ and its ratio with $\mathrm{BR}(H \to \gamma\gamma)$ a stringent test of physics beyond the SM. Similarly, scenarios in which the Higgs boson is composite or arises from alternative symmetry-breaking sectors may yield significantly different $H \to Z\gamma$ branching fractions [20–22].

The $Z(\to \ell\ell)\gamma$ final state ($\ell = e, \mu$), despite its reduced branching ratio, offers the best sensitivity to the $H \to Z\gamma$ process, as it can be efficiently triggered on and clearly distinguished from background events produced in proton–proton (pp) collisions. Furthermore, it benefits from full kinematic reconstruction and excellent invariant mass resolution. Both the ATLAS and CMS Collaborations have performed searches for the $H \to Z(\to \ell\ell)\gamma$ decay using the Run-2 pp collision dataset, corresponding to an integrated luminosity of about 140 fb^{-1} at $\sqrt{s} = 13$ TeV for each experiment. Compared to the background-only hypothesis, ATLAS observed an excess of events at $m_H = 125.09$ GeV with a significance of 2.2σ, while the expectation from the SM is 1.2σ with a measured signal strength, defined by the ratio of the signal yield to the SM prediction, $\mu = 2.0^{+1.0}_{-0.9}$ [23]. Similarly, the CMS Collaboration reported an excess with a significance of 2.7σ (1.2σ expected) with $\mu = 2.4 \pm 0.9$ [24]. The combination of these searches yielded the first evidence of $H \to Z\gamma$ decays with a significance of 3.4σ (1.6σ expected) with $\mu = 2.2 \pm 0.7$ [25]. The combined result is consistent with the SM expectation within two standard deviations.

This letter presents a search for $H \to Z\gamma$ decays in the $\ell\ell\gamma$ final state using pp collision data collected with the ATLAS detector at $\sqrt{s} = 13.6$ TeV during 2022–2024 in Run 3, corresponding to an integrated luminosity of 165 fb^{-1}. Compared to the Run-2 analysis [23], this study benefits from an increased Higgs boson production cross-section at higher centre-of-mass energy, and from a larger data and simulated background samples that improve the description of the expected background distributions in both the multivariate classifications and the background modelling studies by reducing statistical fluctuations and model uncertainty. Furthermore, the event selection is optimised with relaxed transverse-momentum (p_{T}) thresholds for muons and

Contact authors: ATLAS Publications (atlas.publications@cern.ch).
[1] Authors are listed at the end of this paper.

https://doi.org/10.1016/j.physletb.2026.140313
Received 18 July 2025; Received in revised form 27 January 2026; Accepted 24 February 2026
Available online 12 March 2026

photons. The signal is extracted from 13 mutually exclusive event categories including, for the first time, a dedicated multi-lepton category designed to target Higgs boson production in association with a vector boson or top quarks. The remaining 12 categories employ multivariate classifiers based on XGBoost [26] to maximise the sensitivity, replacing the previous approach, mostly based on rectangular selections on simple kinematic variables. A simultaneous fit to the reconstructed $Z\gamma$ invariant mass distributions across all categories is performed to extract the overall $H \to Z\gamma$ signal yield. Finally, the result is combined with the Run-2 measurement to increase the sensitivity to this rare decay.

2. ATLAS detector

The ATLAS experiment [27,28] at the LHC is a multipurpose particle detector with a forward–backward symmetric cylindrical geometry and near 4π coverage in solid angle.[1] It consists of an inner tracking detector (ID) surrounded by a thin superconducting solenoid providing a 2 T axial magnetic field, electromagnetic (EM) and hadronic calorimeters, and a muon spectrometer (MS). The inner tracking detector covers the pseudorapidity range $|\eta| < 2.5$. It consists of silicon pixels, silicon microstrips, and transition radiation tracking detectors. Lead/liquid-argon (LAr) sampling calorimeters provide electromagnetic (EM) energy measurements with high granularity within the region $|\eta| < 3.2$. A steel/scintillator-tile hadronic calorimeter covers the central pseudorapidity range ($|\eta| < 1.7$). The endcap and forward regions are instrumented with LAr calorimeters for EM and hadronic energy measurements up to $|\eta| = 4.9$. The muon spectrometer surrounds the calorimeters and is based on three large superconducting air-core toroidal magnets with eight coils each. The field integral of the toroids ranges between 2.0 and 6.0 T m across most of the detector. The muon spectrometer includes a system of precision tracking chambers up to $|\eta| = 2.7$ and fast detectors for triggering up to $|\eta| = 2.4$. The luminosity is primarily measured by the LUCID-2 detector, which is located close to the beam pipe. A two-level trigger system was used to select events [29,30]. The first-level trigger is implemented in hardware and uses a subset of the detector information to accept events at a rate close to 100 kHz. This is followed by a software-based trigger that reduced the accepted rate of complete events to 3 kHz on average, depending on the data-taking conditions. A software suite [31] is used in data simulation, in the reconstruction and analysis of real and simulated data, in detector operations, and in the trigger and data acquisition systems of the experiment.

3. Data and simulation samples

The analysis presented in this letter uses pp collision data at $\sqrt{s} = 13.6$ TeV collected by the ATLAS experiment from 2022 to 2024 during LHC Run 3. Events were collected using unprescaled single- and dilepton triggers [32,33] with a variety of p_{T} thresholds. The lowest-threshold single-electron and single-muon triggers required $p_{\mathrm{T}} > 26$ GeV and $p_{\mathrm{T}} > 24$ GeV, respectively. The dielectron trigger required two electrons with $p_{\mathrm{T}} > 17$ GeV each. The dimuon triggers employed a symmetric 14 GeV–14 GeV configuration in 2022–2024 and an asymmetric 22 GeV–8 GeV configuration in 2023–2024. To improve the efficiency at high instantaneous luminosity, these low-threshold triggers were supplemented by higher-p_{T} triggers with looser identification or isolation requirements. The trigger selections yield an efficiency of 96% for the $ee\gamma$ final state and 93% for the $\mu\mu\gamma$ final state for events passing the offline selection requirements that will be described in Section 4. After data quality requirements, the total integrated luminosity amounts to 165 fb^{-1}. The average number of inelastic pp interactions per bunch crossing (pile – up) increased from 42 in 2022 to 58 in 2024, with the peak instantaneous luminosity reaching 2.3×10^{34} $\mathrm{cm}^{-2}\mathrm{s}^{-1}$.

The optimisation of the analysis strategy and the modelling of the relevant physics processes rely on simulation Monte Carlo (MC) samples that represent both the Higgs boson signal and the dominant background processes. These samples, unless explicitly stated otherwise, undergo the full simulation of the ATLAS detector response using the GEANT framework [34], as implemented in the ATLAS simulation infrastructure [35]. The Higgs boson mass is set to $m_H = 125$ GeV for all simulated samples, with a corresponding total decay width of $\Gamma_H = 4.1$ MeV, as recommended in Ref. [12]. The simulated samples are normalised to the SM production cross-sections, evaluated at a Higgs boson mass of $m_H = 125.09$ GeV. These include production via gluon–gluon fusion (ggF) [12,36–47], vector boson fusion (VBF) [12,48–50], associated production with a vector boson (VH, where $V = W, Z$) [12,51–58], associated production with a top-quark pair ($t\bar{t}H$) [12,59–62], and associated production with a bottom-quark pair ($b\bar{b}H$) [63–65]. Other Higgs boson production mechanisms were not considered, as their contributions to the total Higgs boson production cross-section are at the level of 0.1% or less. The $H \to Z\gamma$ branching ratio and its uncertainty are also taken from Ref. [12].

The production of the Higgs boson was simulated using the POWHEG BOX v2 MC event generator [66–70] and the PDF4LHC21 parton distribution functions (PDF) set [71], following the setup summarised in Table 1. The $H \to Z\gamma$ decay, as well as parton shower, hadronisation, and the modelling of the underlying event, were performed using PYTHIAV 8 [72]. Contributions from $H \to \mu\mu$ decays, where the reconstructed photon originates from QED final-state radiation (FSR), were evaluated using samples produced with a similar setup and are considered as a potential background in this analysis. The impact of the interference between the signal and other Higgs boson decays with the same final-state signature (e.g. $H \to \gamma\gamma^\star \to \ell\ell\gamma$) is expected to be negligible in the SM [73]. Additional samples of the $H \to Z\gamma$ signals were generated using HERWIGV 7 [74] for decay and parton shower simulation and are used to evaluate uncertainties associated with the parton shower modelling.

In this analysis, the dominant backgrounds arise from non-resonant production of a Z boson in association with a photon ($Z\gamma$) or jets, where a jet is misidentified as a photon (Z+jets). Additional background contributions stem from diboson (VV) production, where V denotes either a W or a Z boson. These additional background contributions are relevant only for the event category containing additional leptons.

A large $Z\gamma$ background sample was generated at next-to-leading-order (NLO) accuracy in QCD using the SHERPAV 2.2.14 generator [75], with one to three additional partons in the final state at LO. The simulation employed the NNPDF 3.0 next-to-next-to-leading-order (NNLO) PDF set [76], and a fast simulation of the calorimeter response was applied [77].

The EW production of a Z boson in association with a photon and two jets ($Z\gamma jj$) was simulated at LO using MADGRAPH 3.5.5 [78] with the NNPDF 2.3LO PDF set [79], where both jets originate from partons emitted at EW vertices. QCD-induced diagrams were explicitly excluded. No additional partons are from QCD interactions in the final state, ensuring orthogonality with the $Z\gamma$ sample generated with SSHERPA. The hadronisation, parton shower, and the modelling of the underlying event were simulated using PYTHIAV 8 with the A14 set of tuned parameters [80].

The background from Z+jets was estimated from data using a control region of events in which the photon candidates fail the nominal criteria and pass looser identification or isolation requirements.

Diboson backgrounds resulting in three- and four-lepton final states were also modelled using SHERPAV 2.2.14, employing the NNPDF

[1] ATLAS uses a right-handed coordinate system with its origin at the nominal interaction point (IP) in the centre of the detector and the z-axis along the beam pipe. The x-axis points from the IP to the centre of the LHC ring, and the y-axis points upwards. Polar coordinates (r, ϕ) are used in the transverse plane, ϕ being the azimuthal angle around the z-axis. The pseudorapidity is defined in terms of the polar angle θ as $\eta = -\ln\tan(\theta/2)$ and is equal to the rapidity $y = \frac{1}{2}\ln\left(\frac{E+p_z}{E-p_z}\right)$ in the relativistic limit. Angular distance is measured in units of $\Delta R \equiv \sqrt{(\Delta y)^2 + (\Delta\phi)^2}$.

Table 1
Higgs boson signal MC samples produced with POWHEG BOX V2 along with the techniques used to generate the events and their precision in α_s for the event generation (gen). The version of PYTHIA V 8.310, A14 tune, and the PDF4LHC21 set, which are used for modelling the Higgs boson decay, parton shower, hadronisation, and the underlying event, are listed. The precision of the total cross-section used in the sample normalisation is also reported.

Process	Technique	QCD (gen.)	Normalisation
ggF*	POWHEG [68,69]	NNLO	N^{3}LO (QCD), NLO (EW) [36–47]
VBF	POWHEG	NLO	NNLO (QCD), NLO (EW) [48–50]
$q\bar{q} \to ZH$	POWHEG& MiNLO [84]	NLO	NNLO (QCD), NLO (EW) [56,58]
$gg \to ZH$	POWHEG	LO	NLO (EW) [58,85,86]
WH	POWHEG& MiNLO [84]	NLO	NNLO (QCD), NLO (EW) [56,58]
$t\bar{t}H$	POWHEG	NLO	NLO (QCD + EW) [59–62,87]
$b\bar{b}H$	POWHEG (4FS)	NLO	NNLO (QCD), NLO (EW) [63–65,88]

* NNLO accuracy achieved only for inclusive ggF observables.

3.0NNLO PDF set. The sample was generated at NLO accuracy in QCD with up to three additional partons at LO accuracy.

The effect of pile – upwas modeled by overlaying simulated hard-scattering events with inelastic pp interactions from a mix of EPOS 2.0.1.4 [81] and PYTHIAV 8. EPOS (PYTHIA) events were generated with the LHC [82] (A3 [83]) tune and NNPDF 2.3LO PDF set. PYTHIA simulated pileup events containing high-p_T jets, prompt photons, or leptons from b-hadron decays, while EPOS accounted for the remaining minimum–bias contribution. The individual samples were first reweighted to ensure a smooth transition across jet p_T, and the combined sample was reweighted to match the distribution of the number of interactions per bunch crossing observed in data.

To improve the agreement between simulation and data, correction factors were applied to account for differences in reconstruction and identification efficiencies. These include corrections to the trigger, reconstruction, identification, and isolation efficiencies for electrons and muons, as well as the identification and selection of photons and jets. Additional corrections were applied to the energy and momentum scale and resolution of reconstructed objects to reflect the detector performance.

4. Event selection and reconstruction

Events passing the trigger selection described in Section 3 are required to include at least one photon and two same-flavour, opposite-charge leptons, all associated with the primary vertex, defined as the inner-detector track vertex with the highest $\sum p_T^2$ of tracks with $p_T >$ 500 MeV [89].

Muon candidates are reconstructed by combining the tracks in the ID and MS [90,91]. They need to satisfy *medium* identification criteria, lie within $|\eta| < 2.5$, and have $p_T > 5$ GeV. Electrons are reconstructed from topological clusters of EM calorimeter cells matched to ID tracks [92–94], incorporating nearby electromagnetic energy deposits associated with bremsstrahlung photons. They are required to pass a *loose* identification selection based on a likelihood discriminant using calorimeter shower shapes and track parameters, lie within $|\eta| < 2.47$ (excluding the transition region between the barrel and endcap EM calorimeters $1.37 < |\eta| < 1.52$), and have $p_T > 10$ GeV. To ensure leptons originate from the primary vertex and to suppress heavy-flavour backgrounds, all leptons are required to satisfy $|\Delta z_0 \cdot \sin\theta| < 0.5$ mm, where Δz_0 is the longitudinal impact parameter relative to the primary vertex and θ is the track polar angle. Moreover, the transverse-impact-parameter significance $|d_0|/\sigma_{d_0}$ needs to be < 3 for muons and < 5 for electrons, with d_0 measured relative to the beam line and σ_{d_0} its fit uncertainty.

Unconverted and converted photon candidates are built from topological clusters of EM calorimeter cells, possibly matched to tracks identified as candidates from $\gamma \to ee$ conversions [92–94]. They have to satisfy *tight* identification criteria based on calorimeter shower shape variables, $|\eta| < 2.37$ (excluding $1.37 < |\eta| < 1.52$), and have $p_T > 10$ GeV (relaxed from 15 GeV in Run 2 [23]). To increase the rejection of background from non-prompt and hadronic production, the lepton and photon candidates are required to pass isolation criteria, based on the energy deposits in the calorimeter and the total p_T of charged-particle tracks from the primary vertex, measured in cones surrounding the direction of the particle candidates.

Jets are reconstructed from particle flow objects [95] clustered via the anti-k_t algorithm ($R = 0.4$) [96–98]. They are required to satisfy $p_T > 25$ GeV and $|y| < 4.4$. To suppress jets originating from pile-up, a central [99] or forward jet-vertex-tagger [100], requiring jets to come from the primary vertex, is applied.

Overlap removal discards the lower-p_T electron when two electron candidates share the same track or satisfy $|\Delta\eta| < 0.075$ and $|\Delta\phi| < 0.125$. Electrons within $\Delta R < 0.02$ of muons are also removed. To suppress bremsstrahlung photons emitted by leptons, photons within $\Delta R < 0.3$ of leptons are discarded. Finally, jets within $\Delta R < 0.2$ of leptons or photons are removed.

Z boson candidates are reconstructed from opposite-charge and same-flavour lepton pairs. In the muon channel, the highest p_T collinear FSR photon ($\Delta R < 0.15$) is added to the corresponding muon to improve the di-muon mass resolution. In the electron channel, the reconstruction and calibration already account for radiative energy losses [93]. A kinematic fit [23] then corrects the lepton four-momenta to constrain the dilepton mass to the known Z boson mass, accounting for its finite natural width. This procedure improves the $\ell\ell\gamma$ mass resolution of the signal MC samples by 17% for electrons and 11% for muons, including the effect of FSR. Candidates must satisfy $|m_{\ell\ell} - m_Z| < 10$ GeV, where $m_Z = 91.2$ GeV [101]. If multiple Z boson candidates are found, the dilepton pair with $m_{\ell\ell}$ closest to m_Z is selected, resulting in a 98% efficiency for correctly matching to the true Z boson in the ggF signal sample. The leptons associated with the Z boson candidate are additionally required to be geometrically matched to the corresponding trigger-level leptons that fired the event. They are required to satisfy an offline p_T threshold set 1–2 GeV above the nominal trigger requirement to ensure that the trigger is maximally efficient.

The Higgs boson candidate is reconstructed by combining the selected Z boson and the highest–p_T photon. The invariant mass of the $\ell\ell\gamma$ system ($m_{Z\gamma}$) must lie within 110–160 GeV to suppress contributions from on-shell Z boson events. In addition, the photon p_T is required to be larger than 0.09 times $m_{Z\gamma}$. This requirement further reduces the background, while not sculpting the $m_{Z\gamma}$ spectrum near m_H as would the use of an absolute minimum p_T^γ requirement with similar background rejection. This criterion is relaxed from the Run-2 value of 0.12 times $m_{Z\gamma}$ thanks to dedicated efficiency corrections and energy calibrations for photons with lower p_T. The overall reconstruction and selection efficiency (including detector acceptance) for the SM $H \to Z(\to \ell\ell)\gamma$ events ranges from 20% to 26%, depending on the production mode.

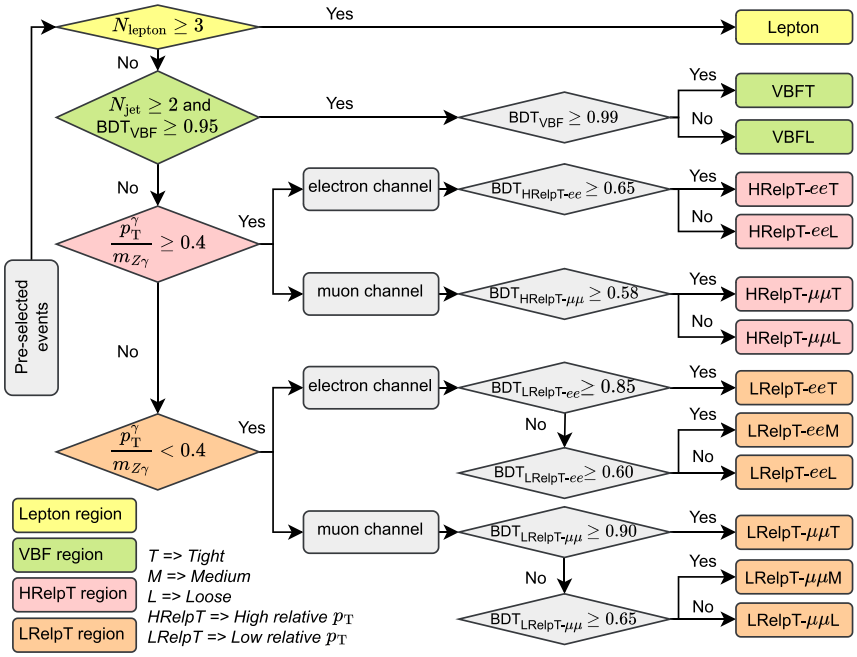

Fig. 1. Schematic of the event categorisation based on kinematic selections and multivariate algorithms. Events are classified into four regions: Lepton (yellow), VBF (green), high relative photon p_{T} (HRelpT, pink), and low relative photon p_{T} (LRelpT, orange). The Lepton region is defined based on the number of lepton candidates, while the VBF region is split into loose and tight categories using a BDT output. The HRelpT and LRelpT regions are further divided into various categories based on the lepton flavour and dedicated BDT classifiers. In total, 13 mutually exclusive categories are defined.

5. Event categorisation

To maximise the sensitivity to an $H \to Z\gamma$ signal, events are classified into 13 exclusive event categories. Events are first categorised into four primary regions based on lepton and jet multiplicities as well as the photon p_{T} relative to $m_{Z\gamma}$: Lepton, VBF, High relative photon p_{T}, and Low relative photon p_{T}. The VBF and both the High and Low relative photon p_{T} regions are further subdivided into mutually exclusive subcategories with different signal purity and roughly similar significance according to the output of an XGBoost-based [26] boosted decision trees (BDT) and to lepton flavour. To avoid sculpting of the $m_{Z\gamma}$ distribution, the BDT inputs are selected to have minimal correlation with $m_{Z\gamma}$, and the classifiers are trained within narrow mass windows around the expected m_H: 120–130 GeV for the VBF and High relative photon p_{T} regions, and 123–127 GeV for the Low relative photon p_{T} region. The number and boundaries of the categories are optimised to maximise the combined expected significance. Each category is required to contain at least two expected background events in the signal region ($120 < m_{Z\gamma} < 130$ GeV). This requirement translates into a minimum number of expected background events in the fit mass region of each category that is large enough to ensure sufficient statistical precision for the background estimate. The event classification scheme is illustrated in Fig. 1, and more details are provided in the following paragraphs.

Events with at least three leptons ($N_{\text{lepton}} \geq 3$) are assigned to the Lepton category. This category is enriched in VH and $t\bar{t}H$ production modes, accounting for 56% and 35% of the signal yield in this category, respectively. The dominant backgrounds arise from Z+jets, multi-lepton diboson, and non-resonant $Z\gamma$processes.

Events failing the Lepton region and containing at least two jets ($N_{\text{jet}} \geq 2$) are selected for the VBF region. If more than two jets are present in an event, the two highest-p_{T} jets are considered. A dedicated BDT was trained using 25 kinematic variables to separate the VBF signal from the non-resonant $Z\gamma$, and the EW $Z\gamma jj$, as well as to reduce the contamination from ggF. The variables are summarised in Table 2. Events in the VBF region are classified into tight (VBFT) and loose (VBFL) categories based on the BDT score, with the VBFT category exhibiting higher significance. The VBF fraction of the total signal yield is 89% and 64%, respectively, in the VBFT and VBFL categories.

Events not selected for the VBF region and satisfying $p_{\text{T}}^{\gamma}/m_{Z\gamma} \geq 0.4$ enter the High relative photon p_{T} region, dominated by ggF production. Separate BDTs are trained for the ee and $\mu\mu$ channels using 17 variables, as shown in Table 2. BDTs are trained using the simulated ggF and VBF signal events and the non-resonant $Z\gamma$ background events. For each lepton flavour, events are grouped into tight and loose categories using optimised BDT thresholds, yielding four categories (HRelpT-eeT, HRelpT-eeL, HRelpT-$\mu\mu$T, HRelpT-$\mu\mu$L) with ggF signal fractions above 70%.

Remaining events that are not selected in the VBF region and with $p_{\text{T}}^{\gamma}/m_{Z\gamma} < 0.4$, are placed into the Low relative photon p_{T} region, where the signal yield is also dominated by ggF with a fraction above 90%. BDTs trained separately for ee and $\mu\mu$ channels use the same input variables as in the High relative photon p_{T} region. The training samples consist of the simulated ggF signal events, the non-resonant $Z\gamma$ background, and the data-driven Z+jets background events. Background components are constructed and normalised as detailed in Section 6. Each channel is split into tight, medium, and loose categories, according to their BDT score, forming six in total: LRelpT – eeT, LRelpT – eeM, LRelpT – eeL, LRelpT-$\mu\mu$T, LRelpT-$\mu\mu$M, and LRelpT-$\mu\mu$L.

Table 3 provides an overview of the expected signal and background composition in each analysis category, as determined from a signal-plus-background fit to the $Z\gamma$ invariant mass distribution of the Asimov dataset (Section 8) to illustrate the sensitivity. The expected signal (S_{68}^{exp}), background (B_{68}^{exp}), and observed data (N_{68}) yields are quoted in an $m_{Z\gamma}$ window around the peak, with a width (w_{68}) corresponding to the interval expected to contain 68% of the signal. The resulting expected sensitivity, $S_{68}^{\text{exp}}/\sqrt{S_{68}^{\text{exp}} + B_{68}^{\text{exp}}}$, varies across categories, reaching a maximum of 0.91 in the VBFT category. The combined sensitivity, obtained by summing the contributions from all categories in quadrature, is 1.81. The inclusive sensitivity is used solely for category optimisation and is not intended to represent the final sensitivity derived from the full statistical analysis.

Table 2
Summary of input variables used in the BDT training for the VBF, HRelpTee, HRelpT$\mu\mu$, LRelpT-ee, and LRelpT-$\mu\mu$ analysis regions. The same set of input variables is employed in the four relative photon p_{T} regions.

Input variable	Description	VBF	relative photon p_{T}
N_{jet}	Number of jets	✓	✓
$p_{\mathrm{T}}^{j_1}$, η_{j_1}	p_{T}, and η of the leading jet (j_1)	✓	✓
m_{j_1}	Mass of the leading jet	✓	
ϕ_{j_1}	Azimuthal angle of the leading jet		✓
m_{j_2}, $p_{\mathrm{T}}^{j_2}$, η_{j_2}	Mass, p_{T}, and η of the subleading jet (j_2)	✓	
$m_{j_1 j_2}$, $p_{\mathrm{T}}^{j_1 j_2}$, $\Delta\eta_{j_1 j_2}$	Dijet invariant mass, p_{T}, and η separation	✓	
η_γ	Pseudorapidity of the photon	✓	✓
p_{T}^γ	Transverse momentum of the photon	✓	
$p_{\mathrm{T}}^{\ell\ell}$	Transverse momentum of the dilepton system	✓	
$\eta_{\ell\ell}$, $\eta_{\ell\ell\gamma}$	Pseudorapidity of the dilepton and $\ell\ell\gamma$ systems	✓	✓
$p_{\mathrm{T}}^{\ell\ell\gamma}$	Transverse momentum of the $\ell\ell\gamma$ system	✓	
$p_{\mathrm{T}}^{\ell\ell\gamma}/m_{\ell\ell\gamma}$, $p_{\mathrm{T}}^{\gamma}/m_{\ell\ell\gamma}$	Relative p_{T} of the $\ell\ell\gamma$ and the photon		✓
$p_{\mathrm{T}}^{\ell\ell}/m_{\ell\ell\gamma}$	Relative p_{T} of the dilepton system		✓
p_t^{T}	Component of $\vec{p}_{\mathrm{T}}^{\,\ell\ell\gamma}$ perpendicular to the difference between $\vec{p}_{\mathrm{T}}^{\,\ell\ell}$ and $\vec{p}_{\mathrm{T}}^{\,\gamma}$ ($p_t^{\mathrm{T}} = \lvert\vec{p}_{\mathrm{T}}^{\,\ell\ell\gamma} \times \hat{t}\rvert$, with $\hat{t} \propto \vec{p}_{\mathrm{T}}^{\,\ell\ell} - \vec{p}_{\mathrm{T}}^{\,\gamma}$) [102,103]	✓	✓
$\Delta\phi_{\ell\ell,\gamma}$	Azimuthal separation between the $\ell\ell$ system and the photon	✓	✓
$\Delta\phi_{\ell\ell\gamma,j_1}$	Azimuthal separation between the $\ell\ell\gamma$ system and the leading jet	✓	✓
$\Delta\phi_{\ell\ell\gamma,j_1 j_2}$	Azimuthal separation between the $\ell\ell\gamma$ system and the dijet system	✓	
$\Delta\eta_{\ell\ell,\gamma}$	Pseudorapidity separation of the dilepton and the photon	✓	✓
$\Delta R_{\gamma \text{ or } \ell\ell,j}^{\mathrm{min}}$	Minimum ΔR to j_1/j_2 from the photon or the dilepton system	✓	✓
$\cos\theta^*(\ell^+)$	Cosine of the polar angle of the ℓ^+ in the $\ell\ell$ rest frame	✓	✓
$\cos\theta(\ell\ell)$ in $\ell\ell\gamma$	Cosine of the polar angle of the $\ell\ell$ in the $\ell\ell\gamma$ rest frame	✓	✓
$\eta^{\mathrm{Zeppenfeld}}$	Pseudorapidity difference between the $\ell\ell\gamma$ system and the dijet system, defined as $\lvert\eta_{\ell\ell\gamma} - (\eta_{j_1} + \eta_{j_2})/2\rvert$ [104]	✓	

Table 3
Expected signal (S_{68}^{exp}), background (B_{68}^{exp}) and observed event yields in data (N_{68}) in a window of width w_{68}, expected to contain 68% of the signal. The expected signal and backgrounds are extracted from a signal-plus-background fit to the Asimov dataset (Section 8). The signal uncertainty reflects the impact in μ, while the background uncertainty accounts for the statistical uncertainty from the fit. The expected sensitivity is given by $S_{68}^{\mathrm{exp}}/\sqrt{S_{68}^{\mathrm{exp}} + B_{68}^{\mathrm{exp}}}$. The last row shows the inclusive results, calculated by summing the contributions from all categories. The inclusive sensitivity is derived by combining the category sensitivities in quadrature.

Category	S_{68}^{exp}	B_{68}^{exp}	N_{68}	w_{68} [GeV]	$S_{68}^{\mathrm{exp}}/\sqrt{S_{68}^{\mathrm{exp}} + B_{68}^{\mathrm{exp}}}$
Lepton	1.5 ± 1.1	75.4 ± 2.8	70	4.4	0.17
VBFT	1.5 ± 1.1	1.3 ± 0.4	3	3.8	0.92
VBFL	2.8 ± 2.0	27.2 ± 1.8	18	4.0	0.52
HRelpT-eeT	1.2 ± 0.8	6.6 ± 0.9	9	3.2	0.43
HRelpT-eeL	2.9 ± 2.1	53.9 ± 1.8	61	4.0	0.39
HRelpT-$\mu\mu$T	2.4 ± 1.7	20.3 ± 1.7	25	3.9	0.51
HRelpT-$\mu\mu$L	2.4 ± 1.7	56.5 ± 1.7	61	4.1	0.32
LRelpT-eeT	8.9 ± 6.2	231 ± 6	240	3.8	0.57
LRelpT-eeM	29 ± 20	$2\,562 \pm 19$	2 587	4.1	0.56
LRelpT-eeL	24 ± 17	$13\,122 \pm 50$	13 074	4.5	0.21
LRelpT-$\mu\mu$T	4.9 ± 3.4	95 ± 4	107	3.9	0.49
LRelpT-$\mu\mu$M	34 ± 24	$2\,527 \pm 19$	2 583	4.1	0.67
LRelpT-$\mu\mu$L	36 ± 25	$16\,844 \pm 40$	16 642	4.4	0.28
Inclusive	150 ± 110	$35\,625 \pm 70$	35 480	4.0	1.81

6. Signal and background modelling

The signal and background yields are determined by an unbinned extended maximum-likelihood fit to the reconstructed $m_{Z\gamma}$ spectrum in data, employing analytic functions for both components. The shape of the $H \to Z\gamma$ signal is modelled by a double-sided Crystal Ball (DSCB) function, comprising a Gaussian core with power-law tails on both sides to capture both the detector resolution and non-Gaussian effects [105]. In each category, the DSCB parameters (mean μ_{CB}, width σ_{CB}, and four parameters describing the tails) are determined from a fit to a combination of all signal samples. The mean is shifted by 90 MeV to correct for the generated Higgs boson mass of 125 GeV to the measured value of 125.09 GeV. The overall signal normalisation and acceptance are taken directly from the same simulation. A small contribution from $H \to \mu\mu$ decays (up to 3.8% of $H \to Z\gamma$ signal in certain categories) is likewise modelled with its own DSCB template, with normalisation fixed to the SM prediction. Depending on the event category, the fitted signal mass resolution ranges from 1.14 to 1.89 GeV.

In each category the background is modelled via an empirical analytical function that is chosen for its ability to provide a precise description of the total background. For all selected events, the backgrounds arise primarily from non-resonant $Z\gamma$ production and Z+jets events in which a jet is misidentified as a photon. The diboson contribution remains below 0.2% and is therefore neglected in the inclusive background estimate. The relative contributions of the $Z\gamma$ and Z+jets backgrounds are obtained inclusively using a two-dimensional sideband (ABCD) method. Four regions are defined by (i) the photon identification requirement, *tight* versus relaxed, and (ii) the isolation requirement, isolated versus non-isolated. The yield of the $Z\gamma$ process in the signal region (*tight* × isolated) is then extracted using the three control regions under the assumption that identification and isolation efficiencies factorise for both background components [106]. This yields a $Z\gamma$ fraction of $0.49^{+0.05}_{-0.10}$, where the uncertainty is derived as the envelope of alternative estimations of the jet background correlations between regions. Compared to $0.78^{+0.04}_{-0.09}$ in Run 2 [23], the reduction reflects three combined effects: the increased pile-up in Run 3, the lowered photon p_{T} threshold in the

Table 4
Breakdown of the symmetrised impacts from individual sources of uncertainty on the expected and observed signal strengths. Uncertainties are grouped by source type to illustrate their relative contributions.

Uncertainty source	$\Delta\mu$ Expected	Observed
Statistical uncertainty	0.68	0.65
Systematic uncertainty	0.16	0.17
Spurious signal (background modelling)	0.11	0.11
QCD scale, PDF + α_S, parton shower	0.09	0.06
Branching ratio ($H \to Z\gamma$)	0.05	0.05
Luminosity	0.03	0.03
Photon efficiency	0.02	0.03
Jet	0.02	0.07
Electron and photon energy scale and resolution	0.02	0.06
Electron efficiency	0.02	0.02
Muon	< 0.01	0.02
Trigger	< 0.01	0.02
Total	0.70	0.67

event selection, which admits more jets faking photons, and the smaller ratio of SM $Z\gamma$ to Z+jets cross-sections at $\sqrt{s} = 13.6$ TeV.

The background $m_{Z\gamma}$ distribution is modelled based on fits to a dedicated background template (the underlying background distribution) that combines the $Z\gamma$ and Z+jets components. After the inclusive fractions of $Z\gamma$ and Z+jets events are determined, they are extrapolated to each event category using efficiencies from the $Z\gamma$ fast-simulation MC and data-driven Z+jets samples. To reduce statistical fluctuations in the control region, the ratio of Z+jets to $Z\gamma$ shapes as a function of $m_{Z\gamma}$ is smoothed by fitting a low-order polynomial or exponential-polynomial function. This smoothed ratio is applied to the $Z\gamma$ template to define the Z+jets background shape. In the VBF categories, a similar smoothing is employed on the ratio of $Z\gamma + (Z + \text{jets})$ to the larger EW $Z\gamma jj$ simulation to define the total background template. In the Lepton category, the 35% contribution from diboson backgrounds, taken from simulation, is added to the template. Finally, in each category, the overall background normalization is scaled to data in the $m_{Z\gamma}$ sidebands (excluding the interval 120–130 GeV). The resulting templates are compatible with the data $m_{Z\gamma}$ distribution, yielding p-values (χ^2) ranging from 1.2% to 78%.

To determine an analytical model that accurately represents the background template without inducing artificial signal features, a spurious signal (SS) study [23] is performed. In each category, several analytic function families, such as power laws, Bernstein polynomials, exponential polynomials, and logarithmic polynomials of the form $(1 - x^{1/3})^f x^{\sum_{i=0}^{N} p_i \log(x)^i}$, with $x = m_{Z\gamma}/\sqrt{s}$ and f a free parameter, are fitted to the background template. Functions in each family are tested over three fit ranges (110–155 GeV, 115–160 GeV, 110–160 GeV). The function-range combinations are required to satisfy two criteria:

- The $|SS|$ is defined as the absolute value of the maximum fitted signal yield obtained from a background-only template when varying m_H between 120 and 130 GeV in steps of 1 GeV. It is required that one of $|SS - 1\sigma|$, SS, or $|SS + 1\sigma|$ is less than $0.2\Delta S$, where σ is the error of the SS, and ΔS is the expected signal statistical uncertainty.
- The χ^2 -probability of the background-only fit > 1%.

When there is more than one function-range combination that passes these criteria, the one with the fewest free parameters is chosen. If more than one has the same number of parameters, the one with the smallest $|SS|$ is chosen. If no candidate satisfies both criteria, the fit window is progressively narrowed (to a minimum width of 35 GeV) until a valid model is found; if still unsuccessful, the combination with the lowest $|SS|$ is adopted. A Wald test [107,108] is then applied to data sidebands to compare nested functions: if a lower-degree function is statistically compatible without significantly increasing $|SS|$, it replaces the nominal model to guard against over-fitting. To account for uncertainties in the relative $Z\gamma$ and Z+jets fractions, variations of those fractions by plus or minus their uncertainties are used to build alternative templates. Repeating the SS study on these templates leaves the chosen function-range combination unchanged in every category, and the maximum $|SS|$ across the three templates is assigned as the systematic uncertainty on the background model.

Once the function is selected, a smoothing technique based on Gaussian Process Regression [108,109] is applied to each category's template. The $|SS|$ is then re-evaluated. This reduces the effect of residual statistical fluctuations without introducing any shape bias and does not affect the choice of any function-range combination in any categories. Unlike the signal models, whose parameters are fixed from simulation, the background model parameters are extracted directly from a fit to the $m_{Z\gamma}$ distribution in data. As an additional validation, a template is built as the sum of the SM signal template and the background template in each category, and is then fitted. The resulting best-fit signal strength in every category is compatible with the SM prediction, confirming the robustness of the background models.

7. Systematic uncertainties

Systematic uncertainties impact the fit results by affecting either the normalization or the shape of the $m_{Z\gamma}$ invariant mass distributions. Experimental uncertainties are evaluated using Run-3 data and MC events. Despite the large simulation background samples and smoothing procedures, the spurious signal, uncorrelated across event categories, retains a large contribution from statistical fluctuations of the input samples. It results in an 11% impact on the signal strength μ, which is small with respect to the statistical uncertainty.

Signal shape modelling uncertainties vary by category and are driven by the calibration of the electron and photon energy, as well as the muon momentum. The uncertainty in the electron and photon energy resolution and in the muon momentum resolution leads to a less than 5% mass resolution (σ_{CB}) uncertainty. The uncertainty in the electron and photon energy scale (and in the muon momentum scale) leads to a less than 0.3% (0.1%) uncertainty in the peak position (μ_{CB}). Overall, these uncertainties affect the measured signal strength by less than 2%.

The 60% uncertainty in the $H \to \mu\mu$ contribution, taken from the Run-2 ATLAS measurement [110], contributes a 2% uncertainty in the expected signal strength. Additional uncertainties in the signal yield arising from reconstruction, identification, and isolation corrections are smaller than 3% for photons, electrons, and muons [93,94]. The jet-related uncertainties, including those from jet reconstruction and in situ calibration, are each below 2%. A conservative uncertainty of 10% is assigned to the reconstruction and calibration of forward jets. All of the jet uncertainties translate into a 4% impact on the signal strength. The uncertainty related to the pile – up effects is negligible. The overall uncertainty in the integrated luminosity for each dataset using the LUCID-2 detector [111] is 4%[2] for 2022–2024. Additional uncertainties arising from the triggers are below 2% across the analysis categories. Combining all experimental systematics, excluding the spurious signal uncertainty, yields a total 9% uncertainty in the signal strength.

Theory uncertainties affecting the expected signal yield arise from multiple sources. Uncertainties in the production cross-section and kinematic distributions, primarily due to missing higher-order QCD corrections, contribute up to 12%, depending on the analysis category, and are dominated by variations in the renormalisation and factorisation scales. The parton shower modelling uncertainty, evaluated by comparing PYTHIA V 8 and HERWIG V 7, ranges from 3% to 29%, with the largest effects observed in the VBF categories. In the non-VBF categories, the

[2] The integrated luminosity for the 2024 dataset is derived from the relative yields of $Z \to ee$ and $Z \to \mu\mu$ events relative to those measured in 2022/2023, yielding a preliminary uncertainty of 5%. When combined with the 2% uncertainty assigned to the 2022/2023 integrated luminosity [112,113], a luminosity-weighted uncertainty of 4% is obtained for the Run-3 dataset.

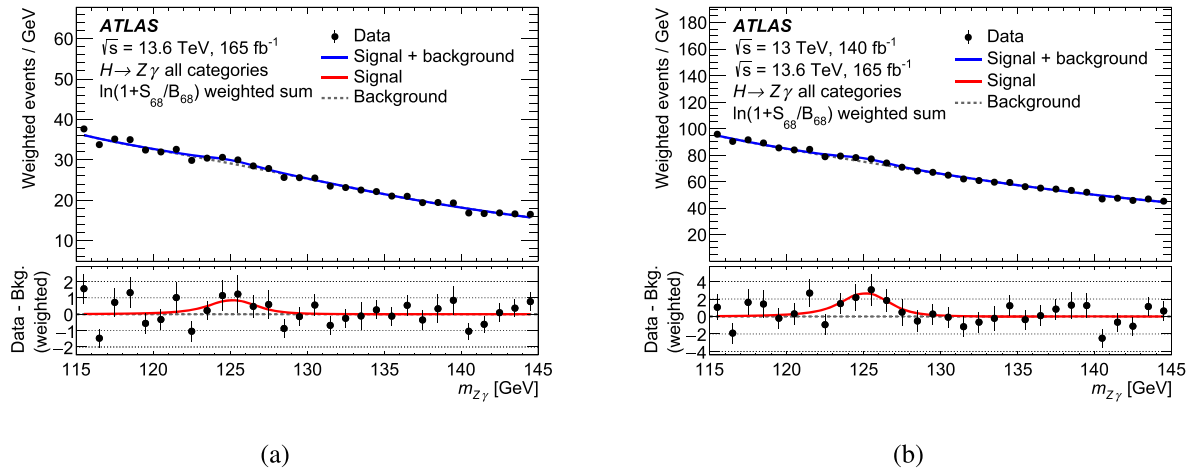

(a) (b)

Fig. 2. $Z\gamma$invariant mass distributions of weighted data events across all categories for (a) Run-3 only and (b) the combined Run-2 and Run-3 dataset. The black points represent the data, with statistical uncertainties shown as error bars. Each event is weighted by $\ln(1 + S_{68}/B_{68})$, where S_{68} and B_{68} are the signal and background yields in each category, estimated from the fit to the data, in an $m_{Z\gamma}$ window expected to contain 68% of the signal. The signal-plus-background fit (solid blue curve) and the background model (dashed line) are overlaid. In the bottom panels, the residuals between the data and the background model (black dots with error bars) are compared to the signal model (red solid line). All curves represent the weighted sum of the individual category models.

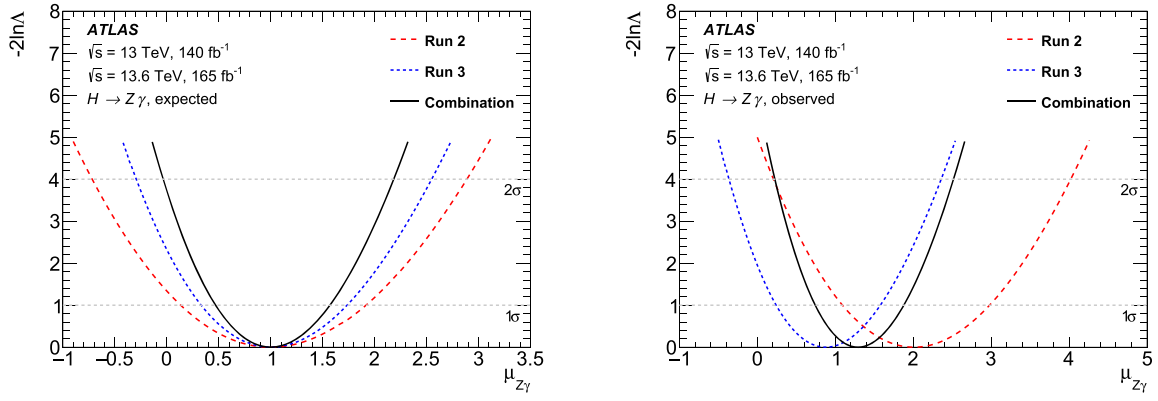

(a) (b)

Fig. 3. Profiled likelihood scan of the signal strength for the (a) expected and (b) observed results. Both plots show the results obtained by this analysis of the Run-3 dataset (dashed blue line), by the previous analysis of the Run-2 dataset [23] (long dashed red line), and their combination (solid black line).

corresponding uncertainty is typically between 0.3% and 10%. The uncertainty in the Higgs boson branching ratio to $Z\gamma$ is 7% [12]. The total impact of theory uncertainties on the signal strength is estimated to be 12%. Table 4 summarises the symmetrised impacts of individual uncertainty sources on the expected and observed signal strengths. The total uncertainty is dominated by the statistical component, with an expected impact of 0.68. Systematic uncertainties contribute 0.16, the spurious signal and theory modelling effects being the leading sources.

8. Results

8.1. Run-3 only

The results are extracted via an unbinned, simultaneous maximum-likelihood fit [114] to the $m_{Z\gamma}$ distributions across all categories, each with its own optimised mass window determined as described in Section 6, following the methodology of previous $H \to Z\gamma$ searches [23, 115]. The likelihood function is built by incorporating both the signal strength of $H \to Z\gamma$ and the nuisance parameters (NPs), which characterise the effects of systematic uncertainties on the signal normalisation and shape, as well as background normalisation and shape parameters.

The measured signal strength is $\mu = 0.9^{+0.7}_{-0.6}(\text{stat.})^{+0.2}_{-0.1}(\text{syst.}) = 0.9^{+0.7}_{-0.6}$ for $m_H = 125.09$ GeV. Under the SM signal hypothesis, the expected signal strength is $\mu_{\text{exp}} = 1.0 \pm 0.7(\text{stat.})^{+0.2}_{-0.1}(\text{syst.}) = 1.0 \pm 0.7$. The corresponding Asimov dataset [114] is generated under the hypothesis of SM signal plus background. The result is statistically compatible with the SM expectation. The observed significance under the background-only hypothesis is 1.4σ, close to the expected significance of 1.5σ. Among the event categories, the VBFT category provides the highest expected sensitivity. In all cases, the uncertainties are dominated by the statistical contribution, while the most significant systematic uncertainty impact arises from the modelling of the background (spurious signal). The measurement using individual signal strengths for each category is consistent with the result obtained from the global signal strength, with a p-value of 0.35.

Fig. 2 (a) presents the $m_{Z\gamma}$ distribution of selected events in the Run-3 dataset, weighted by $\ln(1 + S_{68}/B_{68})$, where S_{68} and B_{68} are the signal and background yields in each category, estimated from the fit to the

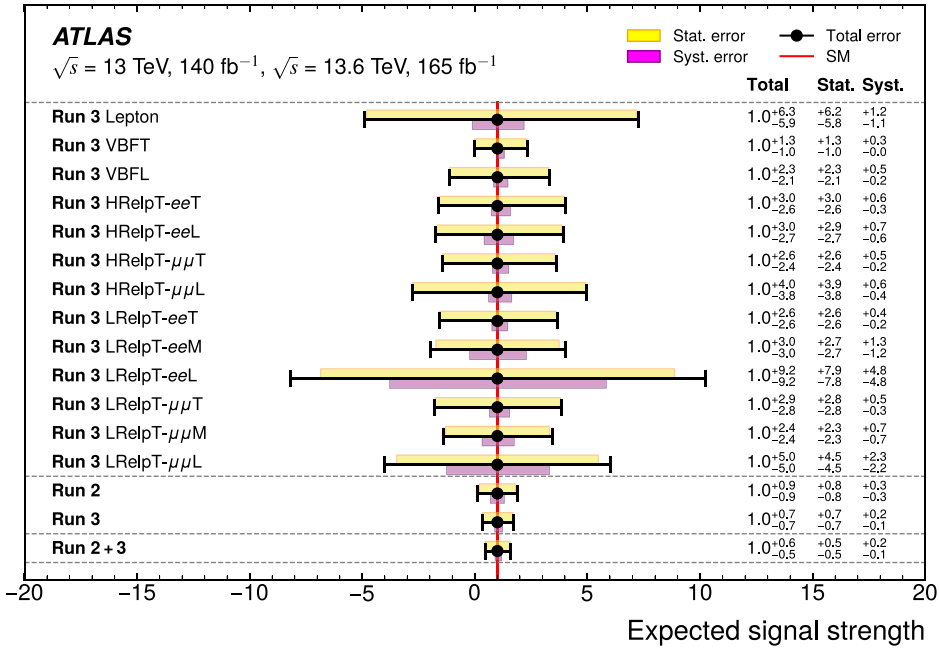

(a)

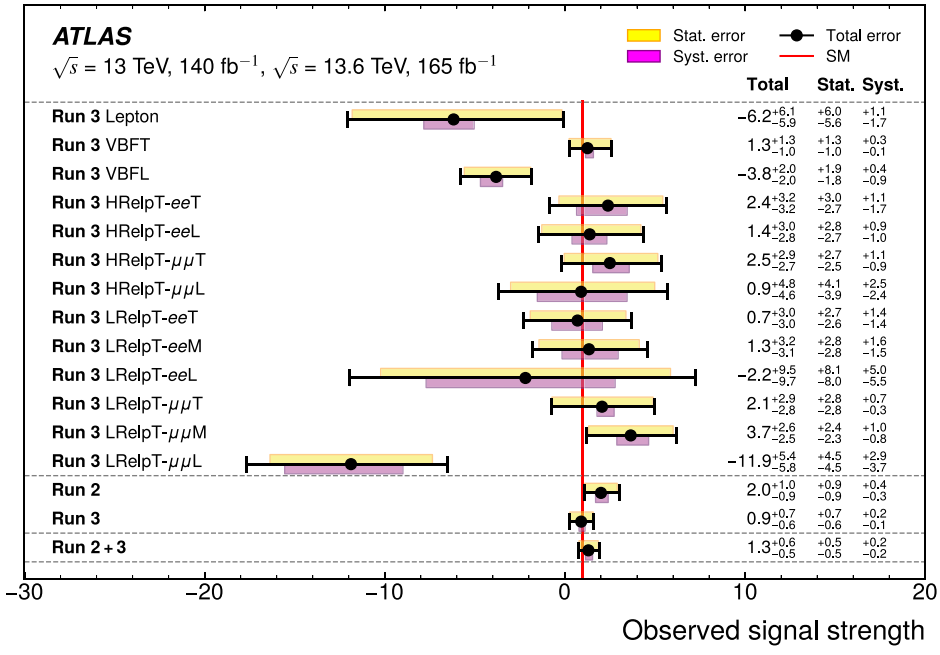

(b)

Fig. 4. (a) Expected and (b) observed best-fit signal strengths and corresponding uncertainties in each category of the Run-3 analysis, their combined values, the results of the previous Run-2 analysis, and the overall combination. The black points with horizontal error bars correspond to the central values and total uncertainties, while the upper yellow (lower magenta) bands indicate the statistical (systematic) uncertainties. The red vertical line denotes the SM prediction.

data, in an $m_{Z\gamma}$ window expected to contain 68% of the signal. The combined models, obtained by weighting the individual category models, are overlaid. The negative profiled-likelihood-ratio values as a function of the signal strength μ are shown in Fig. 3.

Overall, this analysis achieves an expected significance improvement of 27% relative to the previous ATLAS result [23]. This gain is primarily driven by the advanced event selection and categorisation, which contributes 14%. The remaining improvement is from the larger dataset and a more favourable signal-to-background ratio at $\sqrt{s} = 13.6$ TeV.

8.2. Run-2 and Run-3 combination

These results based on Run-3 data are combined with those from the previous ATLAS search for $H \to Z\gamma$ decays using Run-2 data [23]. The theoretical uncertainties, including branching ratios, QCD scale, and α_s uncertainties, are treated as fully correlated across both datasets. The PDF uncertainties are uncorrelated due to the distinct PDF sets used in Run 2 and Run 3. Due to the different data-taking conditions, most experimental uncertainties are treated as uncorrelated between the two

runs, in particular, the uncertainties related to the trigger, luminosity, electron, photon, and spurious signal. All of the uncertainty sources from muons and jets are correlated, except for the uncorrelated in situ calibration uncertainties. The impact of the correlation scheme of systematic uncertainties on the final results was studied and found to be negligible, as the overall uncertainty is dominated by the statistical contributions. The joint likelihood is constructed as the product of the individual likelihood functions from the Run-2 and Run-3 analyses. Correlated systematic sources share a common NP with a Gaussian constraint in the combined fit.

Fig. 2 (b) presents the weighted $m_{Z\gamma}$ distribution with the fitted signal and background models overlaid, and Fig. 3 shows the likelihood scan of the combined signal strength. The observed combined fit has a best-fit signal strength of $\mu = 1.3 \pm 0.5(\text{stat.}) \pm 0.2(\text{syst.}) = 1.3^{+0.6}_{-0.5}$ with an expected $\mu = 1.0 \pm 0.5(\text{stat.})^{+0.2}_{-0.1}(\text{syst.}) = 1.0^{+0.6}_{-0.5}$. The significance of the observed (expected) excess above the background-only hypothesis is 2.5σ (1.9σ). Relative to the Run-2 analysis, the combined expected significance improves by 61%. Fig. 4 shows the signal strength results in each Run-3 category, their combined value, the results of the previous Run-2 analysis, and the overall combination. The Run-2 and Run-3 measurements are compatible, with a p-value of 0.32. Assuming the SM production cross-sections, the combination provides the most stringent expected sensitivity to date for determining the $H \to Z\gamma$ branching fraction, surpassing the ATLAS + CMS Run-2 combination [25]. Under this assumption, the observed (expected) branching fraction is $(2.0^{+0.9}_{-0.8}) \times 10^{-3}$ $((1.5^{+0.9}_{-0.8}) \times 10^{-3})$, compared with the SM prediction of $(1.54^{+0.10}_{-0.11}) \times 10^{-3}$.

9. Conclusion

A search for the Higgs boson decay to $Z\gamma$ in the $\ell\ell\gamma$ final state is performed using proton–proton collision data recorded with the ATLAS detector at $\sqrt{s} = 13.6$ TeV during 2022–2024, corresponding to an integrated luminosity of 165 fb^{-1}. A simultaneous unbinned maximum-likelihood fit to the reconstructed invariant mass of the $Z\gamma$ system across all event categories gives an observed (expected) signal yield normalised to the SM prediction, $\mu = 0.9^{+0.7}_{-0.6}$ ($\mu = 1.0 \pm 0.7$). This corresponds to an observed (expected) signal significance of 1.4 (1.5) standard deviations. The statistical uncertainty is the dominant source of error. Compared to a similar search performed with Run-2 data [23], the expected significance improves by 28%, with 15% arising from the enhanced event selection and categorisation strategies, and the remainder from increased integrated luminosity and larger cross-sections.

This measurement is further combined with the Run-2 result to yield the most stringent expected sensitivity to date for the $H \to Z\gamma$ decay, surpassing the ATLAS + CMS Run-2 combination [25]. In the combined fit, the observed (expected) signal yield normalised to the SM prediction is $\mu = 1.3^{+0.6}_{-0.5}$ ($\mu = 1.0^{+0.6}_{-0.5}$), corresponding to an observed (expected) signal significance of 2.5 (1.9) standard deviations. The combination improves the expected significance by 61% with respect to the Run-2 measurement. The measurement is consistent with the SM expectation, indicating no significant deviation from the predicted Higgs boson behaviour in the $Z\gamma$ channel.

Data availability

The data for this manuscript are not available. The values in the plots and tables associated to this article are stored in HEPDATA (http://hepdata.cedar.ac.uk)"

Declaration of interests

The authors declare that they have no known competing financial interests or personal relationships that could have appeared to influence the work reported in this paper.

Acknowledgements

We thank CERN for the very successful operation of the LHC and its injectors, as well as the support staff at CERN and at our institutions worldwide without whom ATLAS could not be operated efficiently. The crucial computing support from all WLCG partners is acknowledged gratefully, in particular from CERN, the ATLAS Tier-1 facilities at TRIUMF/SFU (Canada), NDGF (Denmark, Norway, Sweden), CC-IN2P3 (France), KIT/GridKA (Germany), INFN-CNAF (Italy), NL-T1 (Netherlands), PIC (Spain), RAL (UK) and BNL (USA), the Tier-2 facilities worldwide and large non-WLCG resource providers. Major contributors of computing resources are listed in Ref. [116]. We gratefully acknowledge the support of ANPCyT, Argentina; YerPhI, Armenia; ARC, Australia; BMWFW and FWF, Austria; ANAS, Azerbaijan; CNPq and FAPESP, Brazil; NSERC, NRC and CFI, Canada; CERN; ANID, Chile; CAS, MOST and NSFC, China; Minciencias, Colombia; MEYS CR, Czech Republic; DNRF and DNSRC, Denmark; IN2P3-CNRS and CEA-DRF/IRFU, France; SRNSFG, Georgia; BMFTR, HGF and MPG, Germany; GSRI, Greece; RGC and Hong Kong SAR, China; ICHEP and Academy of Sciences and Humanities, Israel; INFN, Italy; MEXT and JSPS, Japan; CNRST, Morocco; NWO, Netherlands; RCN, Norway; MNiSW, Poland; FCT, Portugal; MNE/IFA, Romania; MSTDI, Serbia; MSSR, Slovakia; ARIS and MVZI, Slovenia; DSI/NRF, South Africa; MICIU/AEI, Spain; SRC and Wallenberg Foundation, Sweden; SERI, SNSF and Cantons of Bern and Geneva, Switzerland; NSTC, Taipei; TENMAK, Türkiye; STFC/UKRI, United Kingdom; DOE and NSF, United States of America. Individual groups and members have received support from BCKDF, CANARIE, CRC and DRAC, Canada; CERN-CZ, FORTE and PRIMUS, Czech Republic; COST, ERC, ERDF, Horizon 2020, ICSC-NextGenerationEU and Marie Skłodowska-Curie Actions, European Union; Investissements d'Avenir Labex, Investissements d'Avenir Idex and ANR, France; DFG and AvH Foundation, Germany; Herakleitos, Thales and Aristeia programmes co-financed by EU-ESF and the Greek NSRF, Greece; BSF-NSF and MINERVA, Israel; NCN and NAWA, Poland; La Caixa Banking Foundation, CERCA Programme Generalitat de Catalunya and PROMETEO and GenT Programmes Generalitat Valenciana, Spain; Göran Gustafssons Stiftelse, Sweden; The Royal Society and Leverhulme Trust, United Kingdom. In addition, individual members wish to acknowledge support from Australia: Funding agency (AGAUR - 2023 BP 00141); CERN: European Organization for Nuclear Research (CERN DOCT); Chile: Agencia Nacional de Investigación y Desarrollo (FONDECYT 1230812, FONDECYT 1240864, Fondecyt 3240661, Fondecyt Regular 1240721); China: Chinese Ministry of Science and Technology (MOST-2023YFA1605700, MOST-2023YFA1609300), National Natural Science Foundation of China (NSFC - 12175119, NSFC 12275265); Czech Republic: Czech Science Foundation (GACR - 24-11373S), Ministry of Education Youth and Sports (ERC-CZ-LL2327, FORTE CZ.02.01.01/00/22_008/0004632), PRIMUS Research Programme (PRIMUS/21/SCI/017); EU: H2020 European Research Council (ERC - 101002463); European Union: European Research Council (BARD No. 101116429, ERC - 948254, ERC 101089007), European Regional Development Fund (HE COFUND GA No.101081355, ERDF), Horizon 2020 Framework Programme (MUCCA - CHIST-ERA-19-XAI-00), European Union, Future Artificial Intelligence Research (FAIR-NextGenerationEU PE00000013), Italian Center for High Performance Computing, Big Data and Quantum Computing (ICSC, NextGenerationEU); France: Agence Nationale de la Recherche (ANR-21-CE31-0013, ANR-21-CE31-0022, ANR-22-EDIR-0002, ANR-24-CE31-0504-01); Germany: Baden-Württemberg Stiftung (BW Stiftung-Postdoc Eliteprogramme), Deutsche Forschungsgemeinschaft (DFG - 469666862, DFG - CR 312/5-2); China: Research Grants Council (GRF); Italy: Istituto Nazionale di Fisica Nucleare (ICSC, NextGenerationEU), Ministero dell'Università e della Ricerca (NextGenEU 153D23001490006 M4C2.1.1, NextGenEU I53D23000820006 M4C2.1.1, NextGenEU I53D23001490006 M4C2.1.1, SOE2024_0000023); Japan: Japan Society for the Promotion

of Science (JSPS KAKENHI JP22H01227, JSPS KAKENHI JP22H04944, JSPS KAKENHI JP22KK0227, JSPS KAKENHI JP24K23939, JSPS KAKENHI JP24KK0251, JSPS KAKENHI JP25H00650, JSPS KAKENHI JP25H01291, JSPS KAKENHI JP25K01023); Norway: Research Council of Norway (RCN-314472); Poland: Ministry of Science and Higher Education (IDUB AGH, POB8, D4 no 9722), Polish National Science Centre (NCN 2021/42/E/ST2/00350, NCN OPUS 2023/51/B/ST2/02507, NCN OPUS nr 2022/47/B/ST2/03059, NCN UMO-2019/34/E/ST2/00393, UMO-2022/47/O/ST2/00148, UMO-2023/49/B/ST2/04085, UMO-2023/51/B/ST2/00920, UMO-2024/53/N/ST2/00869); Portugal: Foundation for Science and Technology (FCT); Spain: Generalitat Valenciana (ASFAE/2022/008), Ministry of Science and Innovation (MCIN & NextGenEU PCI2022-135018-2, MICIN & FEDER PID2021-125273NB, RYC2019-028510-I, RYC2020-030254-I, RYC2021-031273-I, RYC2022-038164-I), Ministerio de Ciencia, Innovación y Universidades/Agencia Estatal de Investigación (PID2022-142604OB-C22); Sweden: Carl Trygger Foundation (Carl Trygger Foundation CTS 22:2312), Swedish Research Council (Swedish Research Council 2023-04654, VR 2021-03651, VR 2022-03845, VR 2022-04683, VR 2023-03403, VR 2024-05451), Knut and Alice Wallenberg Foundation (KAW 2018.0458, KAW 2022.0358, KAW 2023.0366); Switzerland: Swiss National Science Foundation (SNSF - PCEFP2_194658); United Kingdom: Royal Society (NIF-R1-231091); United States of America: U.S. Department of Energy (ECA DE-AC02-76SF00515), Neubauer Family Foundation.

The ATLAS Collaboration

G. Aad[152], E. Aakvaag[18], B. Abbott[174], S. Abdelhameed[169], K. Abeling[82], N.J. Abicht[76], S.H. Abidi[43], M. Aboelela[71], A. Aboulhorma[60], H. Abramowicz[224], Y. Abulaiti[171], B.S. Acharya[100,101,259], A. Ackermann[91], C. Adam Bourdarios[5], L. Adamczyk[134], S.V. Addepalli[214], M.J. Addison[151], J. Adelman[168], A. Adiguzel[26], T. Adye[194], A.A. Affolder[196], Y. Afik[65], M.N. Agaras[14], A. Aggarwal[150], C. Agheorghiesei[36], F. Ahmadov[64,276], S. Ahuja[145], X. Ai[207], G. Aielli[115,116], A. Aikot[237], M. Ait Tamlihat[60], B. Aitbenchikh[56], M. Akbiyik[150], T.P.A. Åkesson[148], A.V. Akimov[216], D. Akiyama[242], N.N. Akolkar[31], S. Aktas[240], G.L. Alberghi[30], J. Albert[239], U. Alberti[22], P. Albicocco[80], G.L. Albouy[88], S. Alderweireldt[79], Z.L. Alegria[175], M. Aleksa[62], I.N. Aleksandrov[64], C. Alexa[35], T. Alexopoulos[11], F. Alfonsi[30], M. Algren[83], M. Alhroob[241], B. Ali[192], H.M.J. Ali[141,269], S. Ali[45], S.W. Alibocus[142], M. Aliev[49], G. Alimonti[105], W. Alkakhi[82], C. Allaire[97], B.M.M. Allbrooke[217], J.S. Allen[151], J.F. Allen[79], P.P. Allport[23], A. Aloisio[107,108], F. Alonso[140], C. Alpigiani[205], Z.M.K. Alsolami[141], A. Alvarez Fernandez[150], M. Alves Cardoso[83], M.G. Alviggi[107,108], M. Aly[151], Y. Amaral Coutinho[126], A. Ambler[154], C. Amelung[62], M. Amerl[151], C.G. Ames[159], T. Amezza[181], D. Amidei[156], B. Amini[81], K. Amirie[228], A. Amirkhanov[64], S.P. Amor Dos Santos[184], K.R. Amos[237], D. Amperiadou[225], S. An[130], C. Anastopoulos[210], T. Andeen[12], J.K. Anders[142], A.C. Anderson[87], A. Andreazza[105,106], S. Angelidakis[10], A. Angerami[67], A.V. Anisenkov[64], A. Annovi[111], C. Antel[62], E. Antipov[216], M. Antonelli[80], F. Anulli[113], M. Aoki[130], T. Aoki[226], M.A. Aparo[217], L. Aperio Bella[75], M. Apicella[44], C. Appelt[224], A. Apyan[33], M. Arampatzi[11], S.J. Arbiol Val[136], C. Arcangeletti[80], A.T.H. Arce[78], J-F. Arguin[158], S. Argyropoulos[225], J.-H. Arling[75], O. Arnaez[5], H. Arnold[216], G. Artoni[113,114], H. Asada[161], K. Asai[172], S. Asatryan[247], N.A. Asbah[62], R.A. Ashby Pickering[241], A.M. Aslam[145], K. Assamagan[43], R. Astalos[41], K.S.V. Astrand[148], S. Atashi[233], R.J. Atkin[47], H. Atmani[61], P.A. Atmasiddha[182], K. Augsten[192], A.D. Auriol[66], V.A. Austrup[151], A.S. Avad[144], G. Avolio[62], K. Axiotis[83], A. Azzam[14], D. Babal[42], H. Bachacou[195], K. Bachas[225,263], A. Bachiu[55], E. Bachmann[77], M.J. Backes[91], A. Badea[65], T.M. Baer[156], P. Bagnaia[113,114], M. Bahmani[21], D. Bahner[81], K. Bai[177], J.T. Baines[194], L. Baines[144], O.K. Baker[246], E. Bakos[17], D. Bakshi Gupta[9], L.E. Balabram Filho[126], V. Balakrishnan[174], R. Balasubramanian[5], E.M. Baldin[63], P. Balek[134], E. Ballabene[30,29], F. Balli[195], L.M. Baltes[91], W.K. Balunas[46], J. Balz[150], I. Bamwidhi[170], E. Banas[136], M. Bandieramonte[183], A. Bandyopadhyay[31], S. Bansal[31], L. Barak[224], M. Barakat[75], E.L. Barberio[155], D. Barberis[20], M. Barbero[152], M.Z. Barel[167], T. Barillari[160], M-S. Barisits[62], T. Barklow[214], P. Baron[193], D.A. Baron Moreno[151], A. Baroncelli[90], A.J. Barr[180], J.D. Barr[146], F. Barreiro[149], J. Barreiro Guimarães da Costa[15], M.G. Barros Teixeira[184], S. Barsov[63], F. Bartels[91], R. Bartoldus[214], A.E. Barton[141], P. Bartos[41], M. Baselga[76], S. Bashiri[136], A. Bassalat[97,249], M.J. Basso[229], S. Bataju[71], R. Bate[238], R.L. Bates[87], S. Batlamous[149], M. Battaglia[196], D. Battulga[21], M. Bauce[113,114], M. Bauer[121], P. Bauer[31], L.T. Bayer[75], L.T. Bazzano Hurrell[44], J.B. Beacham[160], T. Beau[181], J.Y. Beaucamp[140], P.H. Beauchemin[232], P. Bechtle[31], H.P. Beck[22,262], K. Becker[241], A.J. Beddall[124], V.A. Bednyakov[64], C.P. Bee[216], L.J. Beemster[17], M. Begalli[128], M. Begel[43], J.K. Behr[75], J.F. Beirer[62], F. Beisiegel[31], M. Belfkir[170], G. Bella[224], L. Bellagamba[30], A. Bellerive[55], C.D. Bellgraph[99], P. Bellos[23], K. Beloborodov[63], I. Benaoumeur[23], D. Benchekroun[56], F. Bendebba[56], Y. Benhammou[224], K.C. Benkendorfer[89], L. Beresford[75], M. Beretta[80], E. Bergeaas Kuutmann[235], N. Berger[5], B. Bergmann[192], J. Beringer[19], G. Bernardi[6], C. Bernius[214], F.U. Bernlochner[31], A. Berrocal Guardia[14], T. Berry[145], P. Berta[193], A. Berthold[77], A. Berti[184], R. Bertrand[152], S. Bethke[160], A. Betti[113,114], A.J. Bevan[144], L. Bezio[83], N.K. Bhalla[81], S. Bharthuar[160], S. Bhatta[216], P. Bhattarai[214], Z.M. Bhatti[171], K.D. Bhide[81], V.S. Bhopatkar[175], R.M. Bianchi[183], G. Bianco[30,29], O. Biebel[159], M. Biglietti[117], C.S. Billingsley[71], Y. Bimgdi[61], M. Bindi[82], A. Bingham[245], A. Bingul[25], C. Bini[113,114], G.A. Bird[46], M. Birman[243], M. Biros[193], S. Biryukov[217], T. Bisanz[76], E. Bisceglie[30,29], J.P. Biswal[194], D. Biswas[212], I. Bloch[75], A. Blue[87], U. Blumenschein[144], V.S. Bobrovnikov[64], L. Boccardo[85,84], M. Boehler[81], B. Boehm[240], D. Bogavac[14], A.G. Bogdanchikov[63], L.S. Boggia[181], V. Boisvert[145], P. Bokan[62], T. Bold[134], M. Bomben[6], M. Bona[144], M. Boonekamp[195], A.G. Borbély[87], I.S. Bordulev[63], G. Borissov[141], D. Bortoletto[180], D. Boscherini[30], M. Bosman[14], K. Bouaouda[56], N. Bouchhar[237], L. Boudet[5], J. Boudreau[183], E.V. Bouhova-Thacker[141], D. Boumediene[66], R. Bouquet[85,84], A. Boveia[173], J. Boyd[62], D. Boye[43], I.R. Boyko[64], L. Bozianu[83], J. Bracinik[23], N. Brahimi[5], G. Brandt[245], O. Brandt[46], B. Brau[153], J.E. Brau[177], R. Brener[243], L. Brenner[167], R. Brenner[235], S. Bressler[243], G. Brianti[119,120], D. Britton[87], D. Britzger[160], I. Brock[31], R. Brock[157], G. Brooijmans[67], A.J. Brooks[99], E.M. Brooks[230], E. Brost[43], L.M. Brown[239,229], L.E. Bruce[89], T.L. Bruckler[180], P.A. Bruckman de Renstrom[136], B. Brüers[75], A. Bruni[30], G. Bruni[30], D. Brunner[73,74], M. Bruschi[30], N. Bruscino[113,114], T. Buanes[18], Q. Buat[205], D. Buchin[160], A.G. Buckley[87], O. Bulekov[124], B.A. Bullard[214], S. Burdin[142], C.D. Burgard[76], A.M. Burger[139], B. Burghgrave[9], O. Burlayenko[81], J. Burleson[236], J.C. Burzynski[213], E.L. Busch[67], V. Büscher[150], P.J. Bussey[87], J.M. Butler[32], C.M. Buttar[87], J.M. Butterworth[146], W. Buttinger[194], C.J. Buxo Vazquez[157], A.R. Buzykaev[64], S. Cabrera Urbán[237], L. Cadamuro[97], H. Cai[62], Y. Cai[30,164,29], Y. Cai[162], V.M.M. Cairo[62], O. Cakir[3], N. Calace[62], P. Calafiura[19], G. Calderini[181], P. Calfayan[55], L. Calic[148], G. Callea[87], L.P. Caloba[126], D. Calvet[66], S. Calvet[66], R. Camacho Toro[181], S. Camarda[62], D. Camarero Munoz[33], P. Camarri[115,116], C. Camincher[239], M. Campanelli[146], A. Camplani[68], V. Canale[107,108], A.C. Canbay[3], E. Canonero[145], J. Cantero[237], Y. Cao[236], F. Capocasa[33], M. Capua[70,69], A. Carbone[105,106], R. Cardarelli[115], J.C.J. Cardenas[9], M.P. Cardiff[33], G. Carducci[70,69], T. Carli[62], G. Carlino[107], J.I. Carlotto[14], B.T. Carlson[183,264], E.M. Carlson[239], J. Carmignani[142], L. Carminati[105,106], A. Carnelli[5], M. Carnesale[62], S. Caron[166], E. Carquin[203], I.B. Carr[155], S. Carrá[109,110], G. Carratta[30,29], C. Carrion Martinez[237], A.M. Carroll[177], M.P.

Casado[14,255], P. Casolaro[107,108], M. Caspar[75], W.R. Castiglioni[65], F.L. Castillo[5], L. Castillo Garcia[14], V. Castillo Gimenez[237], N.F. Castro[184,188], A. Catinaccio[62], J.R. Catmore[179], T. Cavaliere[5], V. Cavaliere[43], L.J. Caviedes Betancourt[28], E. Celebi[124], S. Cella[62], V. Cepaitis[83], K. Cerny[176], A.S. Cerqueira[125], A. Cerri[111,285], L. Cerrito[115,116], F. Cerutti[19], B. Cervato[105,106], A. Cervelli[30], G. Cesarini[80], S.A. Cetin[124], P.M. Chabrillat[181], R. Chakkappai[97], S. Chakraborty[241], A. Chambers[89], J. Chan[19], W.Y. Chan[226], J.D. Chapman[46], E. Chapon[195], B. Chargeishvili[221], D.G. Charlton[23], C. Chauhan[193], Y. Che[162], S. Chekanov[7], S.V. Chekulaev[229], G.A. Chelkov[64,248], B. Chen[224], B. Chen[239], H. Chen[162], H. Chen[43], J. Chen[208], J. Chen[213], M. Chen[180], S. Chen[137], S.J. Chen[162], X. Chen[208], X. Chen[16,280], Z. Chen[90], C.L. Cheng[244], H.C. Cheng[93], S. Cheong[214], A. Cheplakov[64], E. Cherepanova[167], R. Cherkaoui El Moursli[60], E. Cheu[8], K. Cheung[96], L. Chevalier[195], V. Chiarella[80], G. Chiarelli[111], G. Chiodini[103], A.S. Chisholm[23], A. Chitan[35], M. Chitishvili[237], M.V. Chizhov[64,265], K. Choi[12], Y. Chou[205], E.Y.S. Chow[166], K.L. Chu[243], M.C. Chu[93], X. Chu[15,164], Z. Chubinidze[80], J. Chudoba[191], J.J. Chwastowski[136], D. Cieri[160], K.M. Ciesla[134], V. Cindro[143], A. Ciocio[19], F. Cirotto[107,108], Z.H. Citron[243], M. Citterio[105], D.A. Ciubotaru[35], A. Clark[83], P.J. Clark[79], N. Clarke Hall[146], C. Clarry[228], S.E. Clawson[75], C. Clement[73,74], Y. Coadou[152], M. Cobal[100,102], A. Coccaro[85], R.F. Coelho Barrue[184], R. Coelho Lopes De Sa[153], S. Coelli[105], L.S. Colangeli[228], B. Cole[67], P. Collado Soto[149], J. Collot[88], R. Coluccia[103,104], P. Conde Muiño[184,190], M.P. Connell[49], S.H. Connell[49], E.I. Conroy[180], M. Contreras Cossio[12], F. Conventi[107,282], A.M. Cooper-Sarkar[180], L. Corazzina[113,114], F.A. Corchia[30,29], A. Cordeiro Oudot Choi[205], L.D. Corpe[66], M. Corradi[113,114], F. Corriveau[154,274], A. Cortes-Gonzalez[226], M.J. Costa[237], F. Costanza[5], D. Costanzo[210], J. Couthures[5], G. Cowan[145], K. Cranmer[244], L. Cremer[76], D. Cremonini[30,29], S. Crépé-Renaudin[88], F. Crescioli[181], T. Cresta[109,110], M. Cristinziani[212], M. Cristoforetti[119,120], E. Critelli[146], V. Croft[167], G. Crosetti[70,69], A. Cueto[149], H. Cui[146], Z. Cui[8], B.M. Cunnett[217], W.R. Cunningham[87], F. Curcio[237], J.R. Curran[79], M.J. Da Cunha Sargedas De Sousa[85,84], J.V. Da Fonseca Pinto[126], C. Da Via[151], W. Dabrowski[134], T. Dado[62], S. Dahbi[219], T. Dai[156], D. Dal Santo[22], C. Dallapiccola[153], M. Dam[68], G. D'amen[43], V. D'Amico[159], J. Damp[150], J.R. Dandoy[55], M. D'Andrea[85,84], D. Dannheim[62], G. D'anniballe[111,112], M. Danninger[213], V. Dao[216], G. Darbo[85], S.J. Das[43], F. Dattola[75], S. D'Auria[105,106], A. D'Avanzo[107,108], T. Davidek[193], J. Davidson[241], I. Dawson[144], K. De[9], C. De Almeida Rossi[228], R. De Asmundis[107], N. De Biase[75], S. De Castro[30,29], N. De Groot[166], P. de Jong[167], H. De la Torre[168], A. De Maria[162], A. De Salvo[113], U. De Sanctis[115,116], F. De Santis[103,104], A. De Santo[217], J.B. De Vivie De Regie[88], J. Debevc[143], D.V. Dedovich[64], J. Degens[142], A.M. Deiana[71], J. Del Peso[149], L. Delagrange[181], F. Deliot[195], C.M. Delitzsch[76], M. Della Pietra[107,108], D. Della Volpe[83], A. Dell'Acqua[62], L. Dell'Asta[105,106], M. Delmastro[5], C.C. Delogu[150], P.A. Delsart[88], S. Demers[246], M. Demichev[64], S.P. Denisov[63], H. Denizli[24,258], L. D'Eramo[66], D. Derendarz[136], F. Derue[181], P. Dervan[142,288], A.M. Desai[1], K. Desch[31], F.A. Di Bello[85,84], A. Di Ciaccio[115,116], L. Di Ciaccio[5], A. Di Domenico[113,114], C. Di Donato[107,108], A. Di Girolamo[62], G. Di Gregorio[62], A. Di Luca[119,120], B. Di Micco[117,118], R. Di Nardo[117,118], K.F. Di Petrillo[65], M. Diamantopoulou[55], F.A. Dias[167], M.A. Diaz[197,198], A.R. Didenko[64], M. Didenko[237], S.D. Diefenbacher[19], E.B. Diehl[156], S. Díez Cornell[75], C. Diez Pardos[212], C. Dimitriadi[215], A. Dimitrievska[23], A. Dimri[216], Y. Ding[90], J. Dingfelder[31], T. Dingley[180], I-M. Dinu[35], S.J. Dittmeier[92], F. Dittus[62], M. Divisek[193], B. Dixit[142], F. Djama[152], T. Djobava[221], C. Doglioni[151,148], A. Dohnalova[41], Z. Dolezal[193], K. Domijan[134], K.M. Dona[65], M. Donadelli[128], B. Dong[157], J. Donini[66], A. D'Onofrio[107,108], M. D'Onofrio[142], J. Dopke[194], A. Doria[107], N. Dos Santos Fernandes[184], I.A. Dos Santos Luz[129], P. Dougan[151], M.T. Dova[140], A.T. Doyle[87], M.P. Drescher[82], E. Dreyer[243], I. Drivas-koulouris[11], M. Drnevich[171], D. Du[90], T.A. du Pree[167], Z. Duan[162], M. Dubau[5], F. Dubinin[64], M. Dubovsky[41], E. Duchovni[243], G. Duckeck[159], P.K. Duckett[146], O.A. Ducu[35], D. Duda[79], A. Dudarev[62], M.M. Dudek[136], E.R. Duden[33], M. D'uffizi[151], L. Duflot[97], M. Dührssen[62], I. Duminica[40], A.E. Dumitriu[35], M. Dunford[91], K. Dunne[73,74], A. Duperrin[152], H. Duran Yildiz[3], A. Durglishvili[221], G.I. Dyckes[19], M. Dyndal[134], B.S. Dziedzic[62], Z.O. Earnshaw[217], G.H. Eberwein[180], B. Eckerova[41], S. Eggebrecht[82], E. Egidio Purcino De Souza[129], G. Eigen[18], K. Einsweiler[19], T. Ekelof[235], P.A. Ekman[148], S. El Farkh[57], Y. El Ghazali[90], H. El Jarrari[62], A. El Moussaouy[56], D. Elitez[62], M. Ellert[235], F. Ellinghaus[245], T.A. Elliot[145], N. Ellis[62], J. Elmsheuser[43], M. Elsawy[169], M. Elsing[62], D. Emeliyanov[194], Y. Enari[130], S. Epari[158], D. Ernani Martins Neto[136], F. Ernst[62], M. Errenst[245], M. Escalier[97], C. Escobar[237], E. Etzion[224], G. Evans[184,185], H. Evans[99], L.S. Evans[75], A. Ezhilov[63], S. Ezzarqtouni[56], F. Fabbri[30,29], L. Fabbri[30,29], G. Facini[146], V. Fadeyev[196], R.M. Fakhrutdinov[63], D. Fakoudis[150], S. Falciano[113], L.F. Falda Ulhoa Coelho[184], F. Fallavollita[160], G. Falsetti[70,69], J. Faltova[193], C. Fan[236], K.Y. Fan[94], Y. Fan[15], Y. Fang[15,164], M. Fanti[105,106], M. Faraj[100,101], Z. Farazpay[147], A. Farbin[9], A. Farilla[117], K. Farman[219], T. Farooque[157], J.N. Farr[246], S.M. Farrington[194,79], F. Fassi[60], D. Fassouliotis[10], L. Fayard[97], P. Federic[193], P. Federicova[191], O.L. Fedin[63,248], M. Feickert[244], L. Feligioni[152], D.E. Fellers[19], C. Feng[206], Y. Feng[15], Z. Feng[167], M.J. Fenton[233], L. Ferencz[75], B. Fernandez Barbadillo[141], P. Fernandez Martinez[98], M.J.V. Fernoux[152], J. Ferrando[141], A. Ferrari[235], P. Ferrari[167,166], R. Ferrari[109], D. Ferrere[83], C. Ferretti[156], M.P. Fewell[1], D. Fiacco[113,114], F. Fiedler[150], P. Fiedler[192], S. Filimonov[64], M.S. Filip[35,266], A. Filipčič[143], E.K. Filmer[229], F. Filthaut[166], M.C.N. Fiolhais[184,186,250], L. Fiorini[237], W.C. Fisher[157], T. Fitschen[151], P.M. Fitzhugh[195], I. Fleck[212], P. Fleischmann[156], T. Flick[245], M. Flores[50,279], L.R. Flores Castillo[93], L. Flores Sanz De Acedo[62], F.M. Follega[119,120], N. Fomin[46], J.H. Foo[228], A. Formica[195], A.C. Forti[151], E. Fortin[62], A.W. Fortman[19], L. Foster[19], L. Fountas[10,256], D. Fournier[97], H. Fox[141], P. Francavilla[111,112], S. Francescato[89], S. Franchellucci[83], M. Franchini[30,29], S. Franchino[91], D. Francis[62], L. Franco[166], L. Franconi[75], M. Franklin[89], G. Frattari[33], Y.Y. Frid[224], J. Friend[87], N. Fritzsche[62], A. Froch[83], D. Froidevaux[62], J.A. Frost[180], Y. Fu[157], S. Fuenzalida Garrido[203], M. Fujimoto[216], K.Y. Fung[93], E. Furtado De Simas Filho[129], M. Furukawa[226], J. Fuster[237], A. Gaa[82], A. Gabrielli[30,29], A. Gabrielli[228], P. Gadow[62], G. Gagliardi[85,84], L.G. Gagnon[19], S. Gaid[132], S. Galantzan[224], J. Gallagher[1], E.J. Gallas[180], A.L. Gallen[235], B.J. Gallop[194], K.K. Gan[173], S. Ganguly[226], Y. Gao[79], Z. Gao[162], A. Garabaglu[205], F.M. Garay Walls[197,198], C. García[237], A. Garcia Alonso[167], A.G. Garcia Caffaro[246], J.E. García Navarro[237], M.A. Garcia Ruiz[28], M. Garcia-Sciveres[19], G.L. Gardner[182], R.W. Gardner[65], N. Garelli[232], R.B. Garg[214], J.M. Gargan[46], C.A. Garner[228], C.M. Garvey[47], V.K. Gassmann[232], G. Gaudio[109], V. Gautam[14], P. Gauzzi[113,114], J. Gavranovic[143], I.L. Gavrilenko[184], A. Gavrilyuk[63], C. Gay[238], G. Gaycken[177], E.N. Gazis[11], A. Gekow[173], C. Gemme[85], M.H. Genest[88], A.D. Gentry[165], S. George[145], T. Geralis[72], A.A. Gerwin[174], P. Gessinger-Befurt[62], M.E. Geyik[245], M. Ghani[241], K. Ghorbanian[144], A. Ghosal[212], A. Ghosh[233], A. Ghosh[8], B. Giacobbe[30], S. Giagu[113,114], T. Giani[167], A. Giannini[90], S.M. Gibson[145], M. Gignac[196], D.T. Gil[135], A.K. Gilbert[134], B.J. Gilbert[67], D. Gillberg[55], G. Gilles[167], D.M. Gingrich[2,281], M.P. Giordani[100,102], P.F. Giraud[195], G. Giugliarelli[100,102], D. Giugni[105], F. Giuli[115,116], I. Gkialas[10,256], L.K. Gladilin[63], C. Glasman[149], M. Glazewska[22], R.M. Gleason[233], G. Glemža[75], M. Glisic[177], I. Gnesi[70], Y. Go[43], M. Goblirsch-Kolb[62], B. Gocke[76], D. Godin[158], B. Gokturk[24], S. Goldfarb[155], T. Golling[83], M.G.D.

Gololo[49], D. Golubkov[63], J.P. Gombas[157], A. Gomes[184,185], G. Gomes Da Silva[212], A.J. Gomez Delegido[62], R. Gonçalo[184], L. Gonella[23], A. Gongadze[222], F. Gonnella[23], J.L. Gonski[214], R.Y. González Andana[79], S. González de la Hoz[237], M.V. Gonzalez Rodrigues[75], R. Gonzalez Suarez[235], S. Gonzalez-Sevilla[83], L. Goossens[62], B. Gorini[62], E. Gorini[103,104], A. Gorišek[143], T.C. Gosart[182], A.T. Goshaw[78], M.I. Gostkin[64], S. Goswami[175], C.A. Gottardo[62], S.A. Gotz[159], M. Gouighri[57], A.G. Goussiou[205], N. Govender[49], R.P. Grabarczyk[180], I. Grabowska-Bold[134], K. Graham[55], E. Gramstad[179], S. Grancagnolo[103,104], C.M. Grant[1], P.M. Gravila[39], F.G. Gravili[103,104], H.M. Gray[19], M. Greco[160], M.J. Green[1], C. Grefe[31], A.S. Grefsrud[18], I.M. Gregor[75], K.T. Greif[233], P. Grenier[214], S.G. Grewe[160], A.A. Grillo[196], K. Grimm[45], S. Grinstein[14,270], J.-F. Grivaz[97], E. Gross[243], J. Grosse-Knetter[82], L. Guan[156], G. Guerrieri[62], R. Guevara[179], R. Gugel[150], J.A.M. Guhit[156], A. Guida[21], E. Guilloton[241], S. Guindon[62], F. Guo[15,164], J. Guo[208], L. Guo[75], L. Guo[163,268], Y. Guo[156], Y. Guo[67], A. Gupta[76], R. Gupta[183], S. Gupta[33], S. Gurbuz[31], S.S. Gurdasani[75], G. Gustavino[113,114], P. Gutierrez[174], L.F. Gutierrez Zagazeta[182], M. Gutsche[77], C. Gutschow[146], C. Gwenlan[180], C.B. Gwilliam[142], E.S. Haaland[179], A. Haas[171], M. Habedank[87], C. Haber[19], H.K. Hadavand[9], A. Haddad[66], A. Hadef[77], A.I. Hagan[141], J.J. Hahn[212], E.H. Haines[146], M. Haleem[240], J. Haley[175], G.D. Hallewell[152], J.A. Hallford[75], K. Hamano[239], H. Hamdaoui[235], M. Hamer[31], S.E.D. Hammoud[97], E.J. Hampshire[145], J. Han[206], L. Han[162], L. Han[90], S. Han[15], K. Hanagaki[130], M. Hance[196], D.A. Hangal[67], H. Hanif[213], M.D. Hank[182], J.B. Hansen[68], P.H. Hansen[68], D. Harada[83], T. Harenberg[245], S. Harkusha[247], M.L. Harris[153], Y.T. Harris[31], J. Harrison[14], N.M. Harrison[173], P.F. Harrison[241], M.L.E. Hart[146], N.M. Hartman[160], N.M. Hartmann[159], R.Z. Hasan[145,194], Y. Hasegawa[211], F. Haslbeck[180], S. Hassan[18], R. Hauser[157], M. Haviernik[193], C.M. Hawkes[23], R.J. Hawkings[62], Y. Hayashi[226], D. Hayden[157], C. Hayes[156], R.L. Hayes[167], C.P. Hays[180], J.M. Hays[144], H.S. Hayward[142], M. He[15,164], Y. He[75], Y. He[146], N.B. Heatley[144], V. Hedberg[148], C. Heidegger[81], K.K. Heidegger[81], J. Heilman[55], S. Heim[75], T. Heim[19], J.J. Heinrich[177], L. Heinrich[160], J. Hejbal[191], M. Helbig[77], A. Held[244], S. Hellesund[18], C.M. Helling[238], S. Hellman[73,74], A.M. Henriques Correia[62], H. Herde[148], Y. Hernández Jiménez[216], L.M. Herrmann[31], T. Herrmann[77], G. Herten[81], R. Hertenberger[159], L. Hervas[62], M.E. Hesping[150], N.P. Hessey[229], J. Hessler[160], M. Hidaoui[57], N. Hidic[193], E. Hill[228], T.S. Hillersoy[18], S.J. Hillier[23], J.R. Hinds[157], F. Hinterkeuser[31], M. Hirose[178], S. Hirose[231], D. Hirschbuehl[245], T.G. Hitchings[151], B. Hiti[143], J. Hobbs[216], R. Hobincu[38], N. Hod[243], A.M. Hodges[236], M.C. Hodgkinson[210], B.H. Hodkinson[180], A. Hoecker[62], D.D. Hofer[156], J. Hofer[237], J. Hofner[150], M. Holzbock[62], L.B.A.H. Hommels[46], V. Homsak[180], B.P. Honan[151], J.J. Hong[99], T.M. Hong[183], B.H. Hooberman[236], W.H. Hopkins[7], M.C. Hoppesch[236], Y. Horii[161], M.E. Horstmann[160], S. Hou[219], M.R. Housenga[236], J. Howarth[87], J. Hoya[7], M. Hrabovsky[176], T. Hryn'ova[5], P.J. Hsu[96], S.-C. Hsu[205], T. Hsu[97], M. Hu[19], Q. Hu[90], S. Huang[46], X. Huang[15,164], Y. Huang[193], Y. Huang[163], Y. Huang[15], Z. Huang[97], Z. Hubacek[192], F. Huegging[31], T.B. Huffman[180], M. Hufnagel Maranha De Faria[125], C.A. Hugli[75], M. Huhtinen[62], S.K. Huiberts[18], R. Hulsken[154], C.E. Hultquist[19], D.L. Humphreys[153], N. Huseynov[13], J. Huston[157], J. Huth[89], L. Huth[75], R. Hyneman[8], G. Iacobucci[83], G. Iakovidis[43], L. Iconomidou-Fayard[97], J.P. Iddon[62], P. Iengo[107,108], R. Iguchi[226], Y. Iiyama[226], T. Iizawa[226], Y. Ikegami[130], D. Iliadis[225], N. Ilic[228], H. Imam[56], G. Inacio Goncalves[128], S.A. Infante Cabanas[199], T. Ingebretsen Carlson[73,74], J.M. Inglis[144], G. Introzzi[109,110], M. Iodice[117], V. Ippolito[113,114], R.K. Irwin[142], M. Ishino[226], W. Islam[244], C. Issever[21], S. Istin[24,287], K. Itabashi[130], H. Ito[242], R. Iuppa[119,120], A. Ivina[243], V. Izzo[107], P. Jacka[192], P. Jackson[1], P. Jain[75], K. Jakobs[81], T. Jakoubek[243], J. Jamieson[87], W. Jang[226], S. Jankovych[193], M. Javurkova[153], P. Jawahar[151], L. Jeanty[177], J. Jejelava[220,277], P. Jenni[81,253], C.E. Jessiman[55], C. Jia[206], H. Jia[238], J. Jia[216], X. Jia[160,164], Z. Jia[162], C. Jiang[79], Q. Jiang[94], S. Jiggins[75], M. Jimenez Ortega[237], J. Jimenez Pena[14], S. Jin[162], A. Jinaru[35], O. Jinnouchi[204], P. Johansson[210], K.A. Johns[8], J.W. Johnson[196], F.A. Jolly[75], D.M. Jones[217], E. Jones[75], K.S. Jones[9], P. Jones[46], R.W.L. Jones[141], T.J. Jones[142], H.L. Joos[82], R. Joshi[173], J. Jovicevic[17], X. Ju[19], J.J. Junggeburth[62], T. Junkermann[91], A. Juste Rozas[14,270], M.K. Juzek[136], S. Kabana[202], A. Kaczmarska[136], S.A. Kadir[214], M. Kado[160], H. Kagan[173], M. Kagan[214], A. Kahn[182], C. Kahra[150], T. Kaji[226], E. Kajomovitz[223], N. Kakati[243], N. Kakoty[14], I. Kalaitzidou[81], S. Kandel[9], N. Kanellos[11], N.J. Kang[196], D. Kar[54,288], E. Karentzos[31], K. Karki[9], O. Karkout[167], S.N. Karpov[64], Z.M. Karpova[64], V. Kartvelishvili[141], A.N. Karyukhin[63], E. Kasimi[225], J. Katzy[75], S. Kaur[55], K. Kawade[211], M.P. Kawale[174], C. Kawamoto[137], T. Kawamoto[90], E.F. Kay[62], F.I. Kaya[232], S. Kazakos[157], V.F. Kazanin[63], J.M. Keaveney[47], R. Keeler[239], G.V. Kehris[89], J.S. Keller[55], J.M. Kelly[239], J.J. Kempster[217], O. Kepka[191], J. Kerr[230], B.P. Kerridge[194], B.P. Kerševan[143], L. Keszeghova[41], R.A. Khan[183], A. Khanov[175], A.G. Kharlamov[63], T. Kharlamova[63], E.E. Khoda[205], M. Kholodenko[184], T.J. Khoo[21], G. Khoriauli[240], Y. Khoulaki[56], Y.A.R. Khwaira[181], B. Kibirige[54], D. Kim[7], D.W. Kim[20], Y.K. Kim[65], N. Kimura[146], M.K. Kingston[82], A. Kirchhoff[82], C. Kirfel[31], F. Kirfel[31], J. Kirk[194], A.E. Kiryunin[160], S. Kita[231], O. Kivernyk[31], M. Klassen[232], C. Klein[55], L. Klein[240], M.H. Klein[71], S.B. Klein[83], U. Klein[142], A. Klimentov[43], T. Klioutchnikova[62], P. Kluit[167], S. Kluth[160], E. Kneringer[121], T.M. Knight[228], A. Knue[76], M. Kobel[77], D. Kobylianskii[243], S.F. Koch[180], M. Kocian[214], P. Kodyš[193], D.M. Koeck[177], T. Koffas[55], O. Kolay[77], I. Koletsou[5], T. Komarek[136], K. Köneke[82], A.X.Y. Kong[1], T. Kono[172], N. Konstantinidis[146], P. Kontaxakis[83], B. Konya[148], R. Kopeliansky[67], S. Koperny[134], K. Korcyl[136], K. Kordas[225,251], A. Korn[146], S. Korn[82], I. Korolkov[14], N. Korotkova[63], B. Kortman[167], O. Kortner[160], S. Kortner[160], W.H. Kostecka[168], M. Kostov[41], V.V. Kostyukhin[212], A. Kotsokechagia[62], A. Kotwal[78], A. Koulouris[62], A. Kourkoumeli-Charalampidi[109,110], C. Kourkoumelis[10], E. Kourlitis[160], O. Kovanda[177], R. Kowalewski[239], W. Kozanecki[177], A.S. Kozhin[63], V.A. Kramarenko[63], G. Kramberger[143], P. Kramer[31], M.W. Krasny[181], A. Krasznahorkay[153], A.C. Kraus[168], J.W. Kraus[245], J.A. Kremer[75], N.B. Krengel[212], T. Kresse[77], L. Kretschmann[245], J. Kretzschmar[142], P. Krieger[228], K. Krizka[23], K. Kroeninger[76], H. Kroha[160], J. Kroll[191], J. Kroll[182], K.S. Krowpman[157], U. Kruchonak[64], H. Krüger[31], N. Krumnack[123], M.C. Kruse[78], O. Kuchinskaia[64], S. Kuday[3], S. Kuehn[62], R. Kuesters[81], T. Kuhl[75], V. Kukhtin[64], Y. Kulchitsky[64], S. Kuleshov[200,198], J. Kull[1], E.V. Kumar[159], M. Kumar[54], N. Kumari[75], P. Kumari[230], A. Kupco[191], A. Kupich[63], O. Kuprash[81], H. Kurashige[133], L.L. Kurchaninov[229], O. Kurdysh[5], Y.A. Kurochkin[63], A. Kurova[63], M. Kuze[204], A.K. Kvam[153], J. Kvita[176], N.G. Kyriacou[205], C. Lacasta[237], F. Lacava[113,114], H. Lacker[21], D. Lacour[181], N.N. Lad[146], E. Ladygin[64], A. Lafarge[66], B. Laforge[181], T. Lagouri[246], F.Z. Lahbabi[56], S. Lai[82,62], W.S. Lai[146], J.E. Lambert[239], S. Lammers[99], W. Lampl[8], C. Lampoudis[225,251], G. Lamprinoudis[240], A.N. Lancaster[168], E. Lançon[43], U. Landgraf[81], M.P.J. Landon[144], V.S. Lang[81], O.K.B. Langrekken[179], A.J. Lankford[233], F. Lanni[62], K. Lantzsch[31], A. Lanza[109], M. Lanzac Berrocal[237], J.F. Laporte[195], T. Lari[105], D. Larsen[18], L. Larson[12], F. Lasagni Manghi[30], M. Lassnig[62], S.D. Lawlor[210], R. Lazaridou[233], M. Lazzaroni[105,106], E.T.T. Le[233], H.D.M. Le[157], E.M. Le Boulicaut[246], L.T. Le Pottier[19], B. Leban[30,29], F. Ledroit-Guillon[88], T.F. Lee[230], L.L. Leeuw[49], M. Lefebvre[239], C. Leggett[19], G. Lehmann Miotto[62], M. Leigh[83], W.A. Leight[153], W. Leinonen[166], A. Leisos[225,267], M.A.L. Leite[127], C.E. Leitgeb[21], R. Leitner[193], K.J.C. Leney[71], T. Lenz[31], S. Leone[111], C. Leonidopoulos[79], A. Leopold[215], J. LePage-Bourbonnais[55], R. Les[157], C.G. Lester[46], M. Levchenko[63], J. Levêque[5], L.J.

Levinson[243], G. Levrini[30,29], M.P. Lewicki[136], C. Lewis[205], D.J. Lewis[5], L. Lewitt[210], A. Li[43], B. Li[206], C. Li[156], C-Q. Li[160], H. Li[206], H. Li[151], H. Li[16], H. Li[90], H. Li[206], J. Li[208], K. Li[15], L. Li[208], R. Li[246], S. Li[15,164], S. Li[209,208], T. Li[6], X. Li[154], Y. Li[15], Z. Li[226], Z. Li[15,164], Z. Li[90], S. Liang[15,164], Z. Liang[15], M. Liberatore[195], B. Liberti[115], G.B. Libotte[128], K. Lie[95], J. Lieber Marin[129], H. Lien[99], H. Lin[156], S.F. Lin[216], L. Linden[159], R.E. Lindley[8], J.H. Lindon[62], J. Ling[89], E. Lipeles[182], A. Lipniacka[18], A. Lister[238], J.D. Little[99], B. Liu[15], B.X. Liu[163], D. Liu[209,208], D. Liu[196], E.H.L. Liu[23], J.K.K. Liu[171], K. Liu[209], K. Liu[209,208], M. Liu[90], M.Y. Liu[90], P. Liu[15], Q. Liu[214,205,208], S. Liu[216], X. Liu[90], X. Liu[206], Y. Liu[163,164], Y. Liu[236], Y.L. Liu[206], Y.W. Liu[90], Z. Liu[97,90], S.L. Lloyd[144], E.M. Lobodzinska[75], P. Loch[8], E. Lodhi[228], K. Lohwasser[210], E. Loiacono[75], J.D. Lomas[23], J.D. Long[67], I. Longarini[233], R. Longo[236], A. Lopez Solis[14], N.A. Lopez-canelas[8], N. Lorenzo Martinez[5], A.M. Lory[159], M. Losada[169], G. Löschcke Centeno[5], X. Lou[73,74], X. Lou[15,164], A. Lounis[97], P.A. Love[141], M. Lu[97], S. Lu[182], Y.J. Lu[219], H.J. Lubatti[205], C. Luci[113,114], F.L. Lucio Alves[162], F. Luehring[99], B.S. Lunday[182], O. Lundberg[215], J. Lunde[62], N.A. Luongo[7], M.S. Lutz[62], A.B. Lux[32], D. Lynn[43], R. Lysak[191], V. Lysenko[192], E. Lytken[148], V. Lyubushkin[64], T. Lyubushkina[64], M.M. Lyukova[216], H. Ma[43], K. Ma[90], L.L. Ma[206], W. Ma[90], Y. Ma[175], J.C. MacDonald[150], P.C. Machado De Abreu Farias[129], D. Macina[62], R. Madar[66], T. Madula[146], J. Maeda[133], T. Maeno[43], P.T. Mafa[49,257], H. Maguire[210], M. Maheshwari[46], V. Maiboroda[97], A. Maio[184,185,187], K. Maj[134], O. Majersky[75], S. Majewski[177], R. Makhmanazarov[63], N. Makovec[97], V. Maksimovic[17], B. Malaescu[181], J. Malamant[179], Pa. Malecki[136], V.P. Maleev[63], F. Malek[88,261], M. Mali[143], D. Malito[145], U. Mallik[122,288], A. Maloizel[6], S. Maltezos[11], A. Malvezzi Lopes[128], S. Malyukov[64], J. Mamuzic[143], G. Mancini[80], M.N. Mancini[33], G. Manco[109,110], J.P. Mandalia[144], S.S. Mandarry[217], I. Mandić[143], L. Manhaes de Andrade Filho[125], I.M. Maniatis[243], J. Manjarres Ramos[139], D.C. Mankad[243], A. Mann[159], T. Manoussos[62], M.N. Mantinan[65], S. Manzoni[62], L. Mao[208], X. Mapekula[49], A. Marantis[225], R.R. Marcelo Gregorio[144], G. Marchiori[6], C. Marcon[105], E. Maricic[17], M. Marinescu[75], S. Marium[75], M. Marjanovic[174], A. Markhoos[81], M. Markovitch[97], M.K. Maroun[153], M.C. Marr[213], G.T. Marsden[151], E.J. Marshall[141], Z. Marshall[19], S. Marti-Garcia[237], J. Martin[146], T.A. Martin[194], V.J. Martin[79], B. Martin dit Latour[18], L. Martinelli[113,114], M. Martinez[14,270], P. Martinez Agullo[237], V.I. Martinez Outschoorn[153], P. Martinez Suarez[62], S. Martin-Haugh[194], G. Martinovicova[193], V.S. Martoiu[35], A.C. Martyniuk[146], A. Marzin[62], D. Mascione[119,120], L. Masetti[150], J. Masik[151], A.L. Maslennikov[64], S.L. Mason[67], P. Massarotti[107,108], P. Mastrandrea[111,112], A. Mastroberardino[70,69], T. Masubuchi[178], T.T. Mathew[177], J. Matousek[193], D.M. Mattern[76], J. Maurer[35], T. Maurin[87], A.J. Maury[97], B. Maček[143], C. Mavungu Tsava[152], D.A. Maximov[63], A.E. May[151], E. Mayer[66], R. Mazini[54], I. Maznas[168], S.M. Mazza[196], E. Mazzeo[62], J.P. Mc Gowan[239], S.P. Mc Kee[156], C.A. Mc Lean[7], C.C. McCracken[238], E.F. McDonald[155], A.E. McDougall[167], L.F. Mcelhinney[141], J.A. Mcfayden[217], R.P. McGovern[182], R.P. Mckenzie[54], T.C. Mclachlan[75], D.J. Mclaughlin[146], S.J. McMahon[194], C.M. Mcpartland[142], R.A. McPherson[239,274], S. Mehlhase[159], A. Mehta[142], D. Melini[237], B.R. Mellado Garcia[54], A.H. Melo[82], F. Meloni[75], A.M. Mendes Jacques Da Costa[151], L. Meng[141], S. Menke[160], M. Mentink[62], E. Meoni[70,69], G. Mercado[168], S. Merianos[225], C. Merlassino[100,102], C. Meroni[105,106], J. Metcalfe[7], A.S. Mete[7], E. Meuser[150], C. Meyer[99], J-P. Meyer[195], Y. Miao[162], R.P. Middleton[194], M. Mihovilovic[97], L. Mijović[79], G. Mikenberg[243], M. Mikestikova[191], M. Mikuž[143], H. Mildner[150], A. Milic[62], D.W. Miller[65], E.H. Miller[214], A. Milov[243], D.A. Milstead[73,74], T. Min[162], A.A. Minaenko[63], I.A. Minashvili[221], A.I. Mincer[171], B. Mindur[134], M. Mineev[64], Y. Mino[137], L.M. Mir[14], M. Miralles Lopez[87], M. Mironova[19], M. Missio[66], A. Mitra[241], V.A. Mitsou[237], Y. Mitsumori[161], O. Miu[228], P.S. Miyagawa[144], T. Mkrtchyan[62], M. Mlinarevic[146], T. Mlinarevic[146], M. Mlynarikova[193], L. Mlynarska[134], C. Mo[208], S. Mobius[22], M.H. Mohamed Farook[165], S. Mohapatra[67], M.F. Mohd Soberi[79], S. Mohiuddin[175], G. Mokgatitswane[54], L. Moleri[243], U. Molinatti[180], L.G. Mollier[22], B. Mondal[191], S. Mondal[192], K. Mönig[75], E. Monnier[152], L. Monsonis Romero[237], J. Montejo Berlingen[14], A. Montella[73,74], M. Montella[173], F. Montereali[117,118], F. Monticelli[140], S. Monzani[100,102], A. Morancho Tarda[68], N. Morange[97], A.L. Moreira De Carvalho[75], M. Moreno Llácer[237], C. Moreno Martinez[83], J.M. Moreno Perez[28], P. Morettini[85], S. Morgenstern[62], M. Morii[89], M. Morinaga[226], M. Moritsu[138], F. Morodei[113,114], P. Moschovakos[62], B. Moser[81], M. Mosidze[221], T. Moskalets[71], P. Moskvitina[166], J. Moss[45], P. Moszkowicz[134], T. Motta Quirino[128], A. Moussa[59], Y. Moyal[243], H. Moyano Gomez[14], E.J.W. Moyse[153], T.G. Mroz[136], O. Mtintsilana[54], S. Muanza[152], M. Mucha[31], J. Mueller[183], G.A. Mullier[235], A.J. Mullin[46], J.J. Mullin[78], A.C. Mullins[71], A.E. Mulski[89], D.P. Mungo[228], D. Munoz Perez[237], F.J. Munoz Sanchez[151], W.J. Murray[241,194], M. Muškinja[143], C. Mwewa[75], A.G. Myagkov[63,248], A.J. Myers[9], G. Myers[156], M. Myska[192], B.P. Nachman[214], K. Nagai[180], K. Nagano[130], R. Nagasaka[226], J.L. Nagle[43,284], E. Nagy[152], A.M. Nairz[62], Y. Nakahama[130], K. Nakamura[130], K. Nakkalil[6], A. Nandi[92], H. Nanjo[178], E.A. Narayanan[71], Y. Narukawa[226], I. Naryshkin[63], L. Nasella[105,106], S. Nasri[170], C. Nass[31], G. Navarro[27], A. Nayaz[21], P.Y. Nechaeva[63], S. Nechaeva[30,29], F. Nechansky[191], L. Nedic[180], T.J. Neep[23], A. Negri[109,110], M. Negrini[30], C. Nellist[167], C. Nelson[154], K. Nelson[156], S. Nemecek[191], M. Nessi[62,254], M.S. Neubauer[236], J. Newell[142], P.R. Newman[23], Y.W.Y. Ng[236], B. Ngair[169], H.D.N. Nguyen[158], J.D. Nichols[174], R.B. Nickerson[180], R. Nicolaidou[195], J. Nielsen[196], M. Niemeyer[82], J. Niermann[62], N. Nikiforou[62], V. Nikolaenko[63,248], I. Nikolic-Audit[181], P. Nilsson[43], I. Ninca[75], G. Ninio[224], A. Nisati[113], R. Nisius[160], N. Nitika[243], J-E. Nitschke[77], E.K. Nkadimeng[48], T. Nobe[226], D. Noll[19], T. Nommensen[218], M.B. Norfolk[210], B.J. Norman[55], L.C. Nosler[19], M. Noury[56], J. Novak[143], T. Novak[143], R. Novotny[192], L. Nozka[176], K. Ntekas[233], D. Ntounis[214], N.M.J. Nunes De Moura Junior[126], J. Ocariz[181], I. Ochoa[184], S. Oerdek[75,271], J.T. Offermann[65], A. Ogrodnik[136], A. Oh[151], C.C. Ohm[215], H. Oide[130], M.L. Ojeda[62], Y. Okumura[226], L.F. Oleiro Seabra[184], I. Oleksiyuk[83], G. Oliveira Correa[14], D. Oliveira Damazio[43], J.L. Oliver[1], R. Omar[99], Ö.O. Öncel[81], A.P. O'Neill[22], A. Onofre[184,188,252], P.U.E. Onyisi[12], M.J. Oreglia[65], D. Orestano[117,118], R. Orlandini[117,118], R.S. Orr[228], L.M. Osojnak[67], Y. Osumi[161], G. Otero y Garzon[44], H. Otono[138], M. Ouchrif[59], F. Ould-Saada[179], T. Ovsiannikova[205], M. Owen[87], R.E. Owen[194], V.E. Ozcan[24], F. Ozturk[136], N. Ozturk[9], S. Ozturk[124], H.A. Pacey[180], K. Pachal[229], A. Pacheco Pages[14], C. Padilla Aranda[14], G. Padovano[113,114], S. Pagan Griso[19], G. Palacino[99], A. Palazzo[103,104], J. Pampel[31], J. Pan[246], T. Pan[93], D.K. Panchal[12], C.E. Pandini[88], J.G. Panduro Vazquez[194], H.D. Pandya[1], H. Pang[195], P. Pani[75], G. Panizzo[100,102], L. Panwar[181], L. Paolozzi[83], S. Parajuli[236], A. Paramonov[7], C. Paraskevopoulos[80], D. Paredes Hernandez[94], S.R. Paredes Saenz[79], A. Pareti[109,110], K.R. Park[67], T.H. Park[160], F. Parodi[85,84], J.A. Parsons[67], U. Parzefall[81], B. Pascual Dias[66], L. Pascual Dominguez[149], E. Pasqualucci[113], S. Passaggio[85], F. Pastore[145], P. Patel[136], U.M. Patel[78], J.R. Pater[151], T. Pauly[62], F. Pauwels[193], C.I. Pazos[232], M. Pedersen[179], R. Pedro[184], S.V. Peleganchuk[63], O. Penc[191], S. Peng[16], G.D. Penn[246], K.E. Penski[159], M. Penzin[63], B.S. Peralva[128], A.P. Pereira Peixoto[205], L. Pereira Sanchez[214], D.V. Perepelitsa[43,284], G. Perera[153], E. Perez Codina[62], M. Perganti[11], H. Pernegger[62], S. Perrella[113,114], K. Peters[75], R.F.Y. Peters[151], B.A. Petersen[62], T.C. Petersen[68], E. Petit[152], V. Petousis[192], A.R. Petri[105,106], C. Petridou[225,251],

T. Petru[193], A. Petrukhin[212], M. Pettee[19], A. Petukhov[124], K. Petukhova[62], R. Pezoa[203], L. Pezzotti[30,29], G. Pezzullo[246], L. Pfaffenbichler[62], A.J. Pfleger[121], T.M. Pham[244], T. Pham[155], P.W. Phillips[194], G. Piacquadio[216], E. Pianori[19], F. Piazza[177], R. Piegaia[44], D. Pietreanu[35], A.D. Pilkington[151], M. Pinamonti[100,102], J.L. Pinfold[2], G. Pinheiro Matos[67], B.C. Pinheiro Pereira[184], J. Pinol Bel[14], A.E. Pinto Pinoargote[181], L. Pintucci[100,102], K.M. Piper[217], A. Pirttikoski[83], D.A. Pizzi[55], L. Pizzimento[94], A. Plebani[46], M.-A. Pleier[43], V. Pleskot[193], E. Plotnikova[64], G. Poddar[144], R. Poettgen[148], L. Poggioli[181], S. Polacek[193], G. Polesello[109], A. Poley[213], A. Polini[30], C.S. Pollard[241], Z.B. Pollock[173], E. Pompa Pacchi[174], N.I. Pond[146], D. Ponomarenko[99], L. Pontecorvo[62], S. Popa[34], G.A. Popeneciu[37], A. Poreba[62], D.M. Portillo Quintero[229], S. Pospisil[192], M.A. Postill[210], P. Postolache[36], K. Potamianos[241], P.A. Potepa[134], I.N. Potrap[64], C.J. Potter[46], H. Potti[218], J. Poveda[237], M.E. Pozo Astigarraga[62], R. Pozzi[62], A. Prades Ibanez[115,116], S.R. Pradhan[210], J. Pretel[239], D. Price[151], M. Primavera[103], L. Primomo[100,102], M.A. Principe Martin[149], R. Privara[176], T. Procter[135], M.L. Proffitt[205], N. Proklova[182], K. Prokofiev[95], G. Proto[160], J. Proudfoot[7], M. Przybycien[134], W.W. Przygoda[135], A. Psallidas[72], J.E. Puddefoot[210], D. Pudzha[80], H.I. Purnell[1], D. Pyatiizbyantseva[166], J. Qian[156], R. Qian[157], D. Qichen[180], Y. Qin[14], T. Qiu[79], A. Quadt[82], M. Queitsch-Maitland[151], G. Quetant[83], R.P. Quinn[238], G. Rabanal Bolanos[89], D. Rafanoharana[160], F. Raffaeli[115,116], F. Ragusa[105,106], J.L. Rainbolt[65], S. Rajagopalan[43], E. Ramakoti[64], L. Rambelli[85,84], I.A. Ramirez-Berend[55], K. Ran[156,164], D.S. Rankin[182], N.P. Rapheeha[54], H. Rasheed[35], D.F. Rassloff[91], A. Rastogi[19], S. Rave[150], S. Ravera[85,84], B. Ravina[62], I. Ravinovich[243], M. Raymond[62], A.L. Read[179], N.P. Readioff[210], D.M. Rebuzzi[109,110], A.S. Reed[87], K. Reeves[33], J.A. Reidelsturz[245], D. Reikher[62], A. Rej[76], C. Rembser[62], H. Ren[90], M. Renda[35], F. Renner[75], A.G. Rennie[87], M. Repik[83], A.L. Rescia[85,84], S. Resconi[105], M. Ressegotti[85], S. Rettie[167], W.F. Rettie[55], M.M. Revering[46], E. Reynolds[19], O.L. Rezanova[64], P. Reznicek[193], H. Riani[59], N. Ribaric[78], B. Ricci[100,102], E. Ricci[119,120], R. Richter[160], S. Richter[73,74], E. Richter-Was[135], M. Ridel[181], S. Ridouani[59], P. Rieck[171], P. Riedler[62], E.M. Riefel[73,74], J.O. Rieger[167], M. Rijssenbeek[216], M. Rimoldi[62], L. Rinaldi[30,29], P. Rincke[235,82], G. Ripellino[235], I. Riu[14], J.C. Rivera Vergara[239], F. Rizatdinova[175], E. Rizvi[144], B.R. Roberts[19], S.S. Roberts[196], D. Robinson[46], M. Robles Manzano[150], A. Robson[87], A. Rocchi[115,116], C. Roda[111,112], S. Rodriguez Bosca[62], Y. Rodriguez Garcia[27], A.M. Rodríguez Vera[168], S. Roe[62], J.T. Roemer[62], O. Røhne[179], R.A. Rojas[62], C.P.A. Roland[181], A. Romaniouk[121], E. Romano[109,110], M. Romano[30], A.C. Romero Hernandez[236], N. Rompotis[142], L. Roos[181], S. Rosati[113], B.J. Rosser[65], E. Rossi[180], E. Rossi[107,108], L.P. Rossi[89], L. Rossini[81], R. Rosten[173], M. Rotaru[35], R. Roth[62], B. Rottler[81], D. Rousseau[97], D. Rousso[75], S. Roy-Garand[228], A. Rozanov[152], Z.M.A. Rozario[87], Y. Rozen[223], A. Rubio Jimenez[237], V.H. Ruelas Rivera[21], T.A. Ruggeri[1], A. Ruggiero[180], A. Ruiz-Martinez[237], A. Rummler[62], Z. Rurikova[81], N.A. Rusakovich[64], S. Ruscelli[76], H.L. Russell[239], G. Russo[113,114], J.P. Rutherfoord[8], S. Rutherford Colmenares[46], M. Rybar[193], P. Rybczynski[134], A. Ryzhov[71], J.A. Sabater Iglesias[83], H.F-W. Sadrozinski[196], F. Safai Tehrani[113], S. Saha[1], M. Sahinsoy[124], B. Sahoo[243], A. Saibel[237], B.T. Saifuddin[174], M. Saimpert[195], G.T. Saito[127], M. Saito[226], T. Saito[226], A. Sala[105,106], A. Salnikov[214], J. Salt[237], A. Salvador Salas[224], F. Salvatore[217], A. Salzburger[62], D. Sammel[81], E. Sampson[141], D. Sampsonidis[225,251], D. Sampsonidou[177], M.A.A. Samy[87], J. Sánchez[237], V. Sanchez Sebastian[237], H. Sandaker[179], C.O. Sander[75], J.A. Sandesara[244], M. Sandhoff[245], C. Sandoval[28], L. Sanfilippo[91], D.P.C. Sankey[194], T. Sano[137], A. Sansoni[80], M. Santana Queiroz[20], L. Santi[62], C. Santoni[66], H. Santos[184,185], A. Santra[243], E. Sanzani[30,29], K.A. Saoucha[132], J.G. Saraiva[184,187], J. Sardain[8], O. Sasaki[130], K. Sato[231], C. Sauer[62], E. Sauvan[5], P. Savard[228,281], R. Sawada[226], C. Sawyer[194], L. Sawyer[147], C. Sbarra[30], A. Sbrizzi[30,29], T. Scanlon[146], J. Schaarschmidt[205], U. Schäfer[150], A.C. Schaffer[97,71], D. Schaile[159], R.D. Schamberger[216], C. Scharf[21], M.M. Schefer[22], V.A. Schegelsky[63], D. Scheirich[193], M. Schernau[202], C. Scheulen[83], C. Schiavi[85,84], M. Schioppa[70,69], B. Schlag[214], S. Schlenker[62], J. Schmeing[245], E. Schmidt[160], M.A. Schmidt[245], K. Schmieden[31], C. Schmitt[150], N. Schmitt[150], S. Schmitt[75], N.A. Schneider[159], L. Schoeffel[195], A. Schoening[92], P.G. Scholer[55], E. Schopf[212], M. Schott[31], S. Schramm[83], T. Schroer[83], H-C. Schultz-Coulon[91], M. Schumacher[81], B.A. Schumm[196], Ph. Schune[195], H.R. Schwartz[8], A. Schwartzman[214], T.A. Schwarz[156], Ph. Schwemling[195], R. Schwienhorst[157], F.G. Sciacca[22], A. Sciandra[43], G. Sciolla[33], F. Scuri[111], C.D. Sebastiani[62], K. Sedlaczek[168], S.C. Seidel[165], A. Seiden[196], B.D. Seidlitz[67], C. Seitz[75], J.M. Seixas[126], G. Sekhniaidze[107], L. Selem[88], N. Semprini-Cesari[30,29], A. Semushin[247], D. Sengupta[83], V. Senthilkumar[237], L. Serin[97], M. Sessa[107,108], H. Severini[174], F. Sforza[85,84], A. Sfyrla[83], Q. Sha[15], E. Shabalina[82], H. Shaddix[168], A.H. Shah[46], R. Shaheen[215], J.D. Shahinian[182], M. Shamim[62], L.Y. Shan[15], M. Shapiro[19], A. Sharma[62], A.S. Sharma[238], P. Sharma[43], P.B. Shatalov[63], K. Shaw[217], S.M. Shaw[151], Q. Shen[15], D.J. Sheppard[213], P. Sherwood[146], L. Shi[146], X. Shi[15], S. Shimizu[130], C.O. Shimmin[246], I.P.J. Shipsey[180,288], S. Shirabe[138], M. Shiyakova[64,272], M.J. Shochet[65], D.R. Shope[179], B. Shrestha[174], S. Shrestha[173,286], I. Shreyber[64], M.J. Shroff[239], P. Sicho[191], A.M. Sickles[236], E. Sideras Haddad[54,234], A.C. Sidley[167], A. Sidoti[30], F. Siegert[77], Dj. Sijacki[17], F. Sili[90], J.M. Silva[79], I. Silva Ferreira[126], M.V. Silva Oliveira[43], S.B. Silverstein[73], S. Simion[97], R. Simoniello[62], E.L. Simpson[151], H. Simpson[217], L.R. Simpson[7], S. Simsek[124], S. Sindhu[82], P. Sinervo[228], S.N. Singh[33], S. Singh[43], S. Sinha[75], S. Sinha[151], M. Sioli[30,29], K. Sioulas[10], I. Siral[62], E. Sitnikova[75], J. Sjölin[73,74], A. Skaf[82], E. Skorda[23], P. Skubic[174], M. Slawinska[136], I. Slazyk[18], I. Sliusar[179], V. Smakhtin[243], B.H. Smart[194], S.Yu. Smirnov[198], Y. Smirnov[124], L.N. Smirnova[63,248], O. Smirnova[148], A.C. Smith[67], D.R. Smith[233], J.L. Smith[151], M.B. Smith[55], R. Smith[214], H. Smitmanns[150], M. Smizanska[141], K. Smolek[192], P. Smolyanskiy[192], A.A. Snesarev[64], H.L. Snoek[167], S. Snyder[43], R. Sobie[239,274], A. Soffer[224], C.A. Solans Sanchez[62], E.Yu. Soldatov[64], U. Soldevila[237], A.A. Solodkov[54], S. Solomon[33], A. Soloshenko[64], K. Solovieva[81], O.V. Solovyanov[66], P. Sommer[77], A. Sonay[14], A. Sopczak[192], A.L. Sopio[79], F. Sopkova[42], J.D. Sorenson[165], I.R. Sotarriva Alvarez[204], V. Sothilingam[91], O.J. Soto Sandoval[199,198], S. Sottocornola[99], R. Soualah[131], Z. Soumaimi[60], D. South[75], N. Soybelman[243], S. Spagnolo[103,104], M. Spalla[160], D. Sperlich[81], B. Spisso[107,108], D.P. Spiteri[87], L. Splendori[152], M. Spousta[193], E.J. Staats[55], R. Stamen[91], E. Stanecka[136], W. Stanek-Maslouska[75], M.V. Stange[77], B. Stanislaus[19], M.M. Stanitzki[75], B. Stapf[75], E.A. Starchenko[63], G.H. Stark[196], J. Stark[139], P. Staroba[191], P. Starovoitov[132], R. Staszewski[136], C. Stauch[159], G. Stavropoulos[72], A. Stefl[62], A. Stein[150], P. Steinberg[43], B. Stelzer[213,229], H.J. Stelzer[183], O. Stelzer[229], H. Stenzel[86], T.J. Stevenson[217], G.A. Stewart[62], J.R. Stewart[175], G. Stoicea[35], M. Stolarski[184], S. Stonjek[160], A. Straessner[77], J. Strandberg[215], S. Strandberg[73,74], M. Stratmann[245], M. Strauss[174], T. Strebler[152], P. Strizenec[42], R. Ströhmer[240], D.M. Strom[177], R. Stroynowski[71], A. Strubig[73,74], S.A. Stucci[43], B. Stugu[18], J. Stupak[174], N.A. Styles[75], D. Su[214], S. Su[90], X. Su[90], D. Suchy[41], A.D. Sudhakar Ponnu[82], K. Sugizaki[182], V.V. Sulin[63], D.M.S. Sultan[180], L. Sultanaliyeva[31], S. Sultansoy[4], S. Sun[244], W. Sun[15], N. Sur[148], M.R. Sutton[217], M. Svatos[191], P.N. Swallow[46], M. Swiatlowski[229], T. Swirski[240], A. Swoboda[62], I. Sykora[41], M. Sykora[193], T. Sykora[193], D. Ta[150], K. Tackmann[75,271], A. Taffard[233], R. Tafirout[229], Y. Takubo[130], M. Talby[152], A.A. Talyshev[63], K.C. Tam[94], N.M. Tamir[224], A. Tanaka[226], J. Tanaka[226], R. Tanaka[97], M. Tanasini[216], Z. Tao[238], S. Tapia Araya[203], S. Tapprogge[150],

A. Tarek Abouelfadl Mohamed[62], S. Tarem[223], K. Tariq[15], G. Tarna[62], G.F. Tartarelli[105], M.J. Tartarin[139], P. Tas[193], M. Tasevsky[191], E. Tassi[70,69], A.C. Tate[236], Y. Tayalati[60,273], G.N. Taylor[155], W. Taylor[230], R.J. Taylor Vara[237], A.S. Tegetmeier[139], P. Teixeira-Dias[145], J.J. Teoh[228], K. Terashi[226], J. Terron[149], S. Terzo[14], M. Testa[80], R.J. Teuscher[228,274], A. Thaler[121], O. Theiner[83], T. Theveneaux-Pelzer[152], D.W. Thomas[145], J.P. Thomas[23], E.A. Thompson[19], P.D. Thompson[23], E. Thomson[182], R.E. Thornberry[71], C. Tian[90], Y. Tian[83], V. Tikhomirov[124], Yu.A. Tikhonov[64], S. Timoshenko[63], D. Timoshyn[193], E.X.L. Ting[1], P. Tipton[246], A. Tishelman-Charny[43], K. Todome[204], S. Todorova-Nova[193], L. Toffolin[100,102], M. Togawa[130], J. Tojo[138], S. Tokár[41], O. Toldaiev[99], G. Tolkachev[152], M. Tomoto[130], L. Tompkins[214,260], E. Torrence[177], H. Torres[139], D.I. Torres Arza[203], E. Torró Pastor[237], M. Toscani[44], C. Tosciri[65], M. Tost[12], D.R. Tovey[210], T. Trefzger[240], P.M. Tricarico[14], A. Tricoli[43], I.M. Trigger[229], S. Trincaz-Duvoid[181], D.A. Trischuk[33], A. Tropina[64], L. Truong[49], M. Trzebinski[136], A. Trzupek[136], F. Tsai[216], M. Tsai[156], A. Tsiamis[225], P.V. Tsiareshka[64], S. Tsigaridas[229], A. Tsirigotis[225,267], V. Tsiskaridze[220], E.G. Tskhadadze[220], Y. Tsujikawa[137], I.I. Tsukerman[63], V. Tsulaia[19], S. Tsuno[130], K. Tsuri[172], D. Tsybychev[216], Y. Tu[94], A. Tudorache[35], V. Tudorache[35], S.B. Tuncay[180], S. Turchikhin[85,84], I. Turk Cakir[3], R. Turra[105], T. Turtuvshin[64,275], P.M. Tuts[67], S. Tzamarias[225,251], Y. Uematsu[130], F. Ukegawa[231], P.A. Ulloa Poblete[199,198], E.N. Umaka[43], G. Unal[62], A. Undrus[43], G. Unel[233], J. Urban[42], P. Urrejola[201], G. Usai[9], R. Ushioda[227], M. Usman[158], F. Ustuner[79], Z. Uysal[124], V. Vacek[192], B. Vachon[154], T. Vafeiadis[62], A. Vaitkus[146], C. Valderanis[159], E. Valdes Santurio[73,74], M. Valente[62], S. Valentinetti[30,29], A. Valero[237], E. Valiente Moreno[237], A. Vallier[139], J.A. Valls Ferrer[237], D.R. Van Arneman[167], A. Van Der Graaf[76], H.Z. Van Der Schyf[54], P. Van Gemmeren[7], M. Van Rijnbach[62], S. Van Stroud[146], I. Van Vulpen[167], P. Vana[193], M. Vanadia[115,116], U.M. Vande Voorde[215], W. Vandelli[62], E.R. Vandewall[175], D. Vannicola[224], L. Vannoli[80], R. Vari[113], M. Varma[246], E.W. Varnes[8], C. Varni[168], D. Varouchas[97], L. Varriale[237], K.E. Varvell[218], M.E. Vasile[35], L. Vaslin[130], M.D. Vassilev[214], A. Vasyukov[64], L.M. Vaughan[175], R. Vavricka[193], T. Vazquez Schroeder[14], J. Veatch[45], V. Vecchio[151], M.J. Veen[153], I. Veliscek[43], I. Velkovska[143], L.M. Veloce[228], F. Veloso[184,186], S. Veneziano[113], A. Ventura[103,104], A. Verbytskyi[160], M. Verducci[111,112], C. Vergis[144], M. Verissimo De Araujo[126], W. Verkerke[167], J.C. Vermeulen[167], C. Vernieri[214], M. Vessella[233], M.C. Vetterli[213,281], A. Vgenopoulos[150], N. Viaux Maira[203,278], T. Vickey[210], O.E. Vickey Boeriu[210], G.H.A. Viehhauser[180], L. Vigani[92], M. Vigl[160], M. Villa[30,29], M. Villaplana Perez[237], E.M. Villhauer[65], E. Vilucchi[80], M. Vincent[237], M.G. Vincter[55], A. Visibile[167], A. Visive[167], C. Vittori[62], I. Vivarelli[30,29], M.I. Vivas Albornoz[75], E. Voevodina[160], F. Vogel[159], J.C. Voigt[77], P. Vokac[192], Yu. Volkotrub[135], L. Vomberg[31], E. Von Toerne[31], B. Vormwald[62], K. Vorobev[78], M. Vos[237], K. Voss[212], M. Vozak[62], L. Vozdecky[174], N. Vranjes[17], M. Vranjes Milosavljevic[17], M. Vreeswijk[167], N.K. Vu[209,208], R. Vuillermet[62], O. Vujinovic[150], I. Vukotic[65], I.K. Vyas[55], J.F. Wack[46], S. Wada[231], C. Wagner[214], J.M. Wagner[19], W. Wagner[245], S. Wahdan[245], H. Wahlberg[140], C.H. Waits[174], J. Walder[194], R. Walker[159], K. Walkingshaw Pass[87], W. Walkowiak[212], A. Wall[182], E.J. Wallin[148], T. Wamorkar[19], K. Wandall-Christensen[237], A. Wang[90], A.Z. Wang[196], C. Wang[150], C. Wang[12], H. Wang[19], J. Wang[95], P. Wang[151], P. Wang[146], R. Wang[89], R. Wang[7], S.M. Wang[219], S. Wang[15], T. Wang[166], T. Wang[90], W.T. Wang[180], W. Wang[15], X. Wang[236], X. Wang[208], X. Wang[75], Y. Wang[162], Y. Wang[90], Z. Wang[156], Z. Wang[209], Z. Wang[156], Z. Wang[15], C. Wanotayaroj[130], A. Warburton[154], A.L. Warnerbring[212], S. Waterhouse[145], A.T. Watson[23], H. Watson[79], M.F. Watson[23], E. Watton[62], G. Watts[205], B.M. Waugh[146], J.M. Webb[81], C. Weber[43], H.A. Weber[21], M.S. Weber[22], S.M. Weber[91], C. Wei[90], Y. Wei[81], A.R. Weidberg[180], E.J. Weik[171], J. Weingarten[76], C. Weiser[81], C.J. Wells[75], T. Wenaus[43], T. Wengler[62], N.S. Wenke[160], N. Wermes[31], M. Wessels[91], A.M. Wharton[141], A.S. White[89], A. White[9], M.J. White[1], D. Whiteson[233], L. Wickremasinghe[178], W. Wiedenmann[244], M. Wielers[194], R. Wierda[215], C. Wiglesworth[68], H.G. Wilkens[62], J.J.H. Wilkinson[46], D.M. Williams[67], H.H. Williams[182], S. Williams[46], S. Willocq[153], B.J. Wilson[151], D.J. Wilson[151], P.J. Windischhofer[65], F.I. Winkel[44], F. Winklmeier[177], B.T. Winter[81], M. Wittgen[214], M. Wobisch[147], T. Wojtkowski[88], Z. Wolffs[167], J. Wollrath[62], M.W. Wolter[136], H. Wolters[184,186], M.C. Wong[196], E.L. Woodward[67], S.D. Worm[75], B.K. Wosiek[136], K.W. Woźniak[136], S. Wozniewski[82], K. Wraight[87], C. Wu[228], C. Wu[23], J. Wu[226], M. Wu[163], M. Wu[166], S.L. Wu[244], S. Wu[15,283], X. Wu[90], Y.Q. Wu[228], Y. Wu[90], Z. Wu[5], Z. Wu[162], J. Wuerzinger[160], T.R. Wyatt[151], B.M. Wynne[79], S. Xella[68], L. Xia[162], M. Xie[90], A. Xiong[177], D. Xu[15], H. Xu[90], L. Xu[90], R. Xu[182], T. Xu[156], Y. Xu[205], Z. Xu[79], R. Xue[183], B. Yabsley[218], S. Yacoob[47], Y. Yamaguchi[130], E. Yamashita[226], H. Yamauchi[231], T. Yamazaki[19], Y. Yamazaki[133], S. Yan[87], Z. Yan[153], H.J. Yang[208,209], H.T. Yang[90], S. Yang[90], T. Yang[95], X. Yang[62], X. Yang[15], Y. Yang[226], Y. Yang[90], W-M. Yao[19], C.L. Yardley[217], J. Ye[15], S. Ye[43], X. Ye[90], Y. Yeh[146], I. Yeletskikh[64], B. Yeo[20], M.R. Yexley[146], T.P. Yildirim[180], K. Yorita[242], C.J.S. Young[62], C. Young[214], N.D. Young[177], Y. Yu[90], J. Yuan[15,164,283], M. Yuan[156], R. Yuan[209,208], L. Yue[146], M. Zaazoua[90], B. Zabinski[136], I. Zahir[56], A. Zaio[85,84], Z.K. Zak[136], T. Zakareishvili[237], S. Zambito[83], J.A. Zamora Saa[200], J. Zang[226], R. Zanzottera[105,106], O. Zaplatilek[192], C. Zeitnitz[245], H. Zeng[15], J.C. Zeng[236], D.T. Zenger Jr[33], O. Zenin[63], T. Ženiš[41], S. Zenz[144], D. Zerwas[97], M. Zhai[15,164], D.F. Zhang[210], G. Zhang[15,283], J. Zhang[206], J. Zhang[7], K. Zhang[15,164], L. Zhang[90], L. Zhang[162], P. Zhang[15,164], R. Zhang[162], S. Zhang[139], T. Zhang[226], Y. Zhang[205], Y. Zhang[146], Y. Zhang[90], Y. Zhang[162], Z. Zhang[19], Z. Zhang[206], Z. Zhang[97], H. Zhao[205], T. Zhao[206], Y. Zhao[55], Z. Zhao[90], Z. Zhao[90], A. Zhemchugov[64], J. Zheng[162], K. Zheng[236], X. Zheng[90], Z. Zheng[214], D. Zhong[236], B. Zhou[156], H. Zhou[8], N. Zhou[208], Y. Zhou[16], Y. Zhou[162], Y. Zhou[8], C.G. Zhu[206], J. Zhu[156], X. Zhu[209], Y. Zhu[208], Y. Zhu[90], X. Zhuang[15], K. Zhukov[99], N.I. Zimine[64], J. Zinsser[92], M. Ziolkowski[212], L. Živković[17], A. Zoccoli[30,29], K. Zoch[89], A. Zografos[62], T.G. Zorbas[210], O. Zormpa[72], L. Zwalinski[62]

Collaboration Institutes

[1] Department of Physics, University of Adelaide, Adelaide, Australia
[2] Department of Physics, University of Alberta, Edmonton, AB, Canada
[3] Department of Physics, Ankara University, Ankara, Türkiye
[4] Division of Physics, TOBB University of Economics and Technology, Ankara, Türkiye
[5] LAPP, Université Savoie Mont Blanc, CNRS/IN2P3, Annecy, France
[6] APC, Université Paris Cité, CNRS/IN2P3, Paris, France
[7] High Energy Physics Division, Argonne National Laboratory, Argonne, IL, United States of America
[8] Department of Physics, University of Arizona, Tucson, AZ, United States of America
[9] Department of Physics, University of Texas at Arlington, Arlington, TX, United States of America
[10] Physics Department, National and Kapodistrian University of Athens, Athens, Greece
[11] Physics Department, National Technical University of Athens, Zografou, Greece
[12] Department of Physics, University of Texas at Austin, Austin, TX, United States of America
[13] Institute of Physics, Azerbaijan Academy of Sciences, Baku, Azerbaijan

[14] Institut de Física d'Altes Energies (IFAE), Barcelona Institute of Science and Technology, Barcelona, Spain
[15] Institute of High Energy Physics, Chinese Academy of Sciences, Beijing, China
[16] Physics Department, Tsinghua University, Beijing, China
[17] Institute of Physics, University of Belgrade, Belgrade, Serbia
[18] Department for Physics and Technology, University of Bergen, Bergen, Norway
[19] Physics Division, Lawrence Berkeley National Laboratory, Berkeley, CA, United States of America
[20] University of California, Berkeley, CA, United States of America
[21] Institut für Physik, Humboldt Universität zu Berlin, Berlin, Germany
[22] Albert Einstein Center for Fundamental Physics and Laboratory for High Energy Physics, University of Bern, Bern, Switzerland
[23] School of Physics and Astronomy, University of Birmingham, Birmingham, United Kingdom
[24] Department of Physics, Bogazici University, Istanbul, Türkiye
[25] Department of Physics Engineering, Gaziantep University, Gaziantep, Türkiye
[26] Department of Physics, Istanbul University, Istanbul, Türkiye
[27] Facultad de Ciencias y Centro de Investigaciónes, Universidad Antonio Nariño, Bogotá, Colombia
[28] Departamento de Física, Universidad Nacional de Colombia, Bogotá, Colombia
[29] Dipartimento di Fisica e Astronomia A. Righi, Università di Bologna, Bologna, Italy
[30] INFN Sezione di Bologna, Italy
[31] Physikalisches Institut, Universität Bonn, Bonn, Germany
[32] Department of Physics, Boston University, Boston, MA, United States of America
[33] Department of Physics, Brandeis University, Waltham, MA, United States of America
[34] Transilvania University of Brasov, Brasov, Romania
[35] Horia Hulubei National Institute of Physics and Nuclear Engineering, Bucharest, Romania
[36] Department of Physics, Alexandru Ioan Cuza University of Iasi, Iasi, Romania
[37] Development of Isotopic and Molecular Technologies, Physics Department, National Institute for Research, Cluj-Napoca, Romania
[38] National University of Science and Technology Politechnica, Bucharest, Romania
[39] West University in Timisoara, Timisoara, Romania
[40] Faculty of Physics, University of Bucharest, Bucharest, Romania
[41] Faculty of Mathematics, Physics and Informatics, Comenius University, Bratislava, Slovak Republic
[42] Department of Subnuclear Physics, Institute of Experimental Physics, Slovak Academy of Sciences, Kosice, Slovak Republic
[43] Physics Department, Brookhaven National Laboratory, Upton, NY, United States of America
[44] Facultad de Ciencias Exactas y Naturales, Departamento de Física, Instituto de Física de Buenos Aires (IFIBA), CONICET, Universidad de Buenos Aires, Buenos Aires, Argentina
[45] California State University, CA, United States of America
[46] Cavendish Laboratory, University of Cambridge, Cambridge, United Kingdom
[47] Department of Physics, University of Cape Town, Cape Town, South Africa
[48] iThemba Labs, Western Cape, South Africa
[49] Department of Mechanical Engineering Science, University of Johannesburg, Johannesburg, South Africa
[50] National Institute of Physics, University of The Philippines Diliman, Philippines
[51] Department of Physics, Stellenbosch University, Matieland, South Africa
[52] Department of Physics, University of South Africa, Pretoria, South Africa
[53] University of Zululand, KwaDlangezwa, South Africa
[54] School of Physics, University of the Witwatersrand, Johannesburg, South Africa
[55] Department of Physics, Carleton University, Ottawa, ON, Canada
[56] Faculté des Sciences Ain Chock, Université Hassan II de Casablanca, Morocco
[57] Faculté des Sciences, Université Ibn-Tofail, Kénitra, Morocco
[58] Faculté des Sciences Semlalia, Université Cadi Ayyad, LPHEA-Marrakech, Morocco
[59] Faculté des Sciences, LPMR, Université Mohamed Premier, Oujda, Morocco
[60] Faculté des sciences, Université Mohammed V, Rabat, Morocco
[61] Institute of Applied Physics, Mohammed VI Polytechnic University, Ben Guerir, Morocco
[62] CERN, Geneva, Switzerland
[63] Affiliated with an institute formerly covered by a cooperation agreement with CERN
[64] Affiliated with an international laboratory covered by a cooperation agreement with CERN
[65] Enrico Fermi Institute, University of Chicago, Chicago, IL, United States of America
[66] LPC, Université Clermont Auvergne, CNRS/IN2P3, Clermont-Ferrand, France
[67] Nevis Laboratory, Columbia University, Irvington, NY, United States of America
[68] Niels Bohr Institute, University of Copenhagen, Copenhagen, Denmark
[69] Dipartimento di Fisica, Università della Calabria, Rende, Italy
[70] INFN Gruppo Collegato di Cosenza, Laboratori Nazionali di Frascati, Italy
[71] Physics Department, Southern Methodist University, Dallas, TX, United States of America
[72] National Centre for Scientific Research Demokritos, Agia Paraskevi, Greece
[73] Department of Physics, Stockholm University, Sweden
[74] Oskar Klein Centre, Stockholm, Sweden
[75] Deutsches Elektronen-Synchrotron DESY, Hamburg and Zeuthen, Germany
[76] Fakultät Physik, Technische Universität Dortmund, Dortmund, Germany
[77] Institut für Kern- und Teilchenphysik, Technische Universität Dresden, Dresden, Germany
[78] Department of Physics, Duke University, Durham, NC, United States of America
[79] SUPA - School of Physics and Astronomy, University of Edinburgh, Edinburgh, United Kingdom
[80] INFN e Laboratori Nazionali di Frascati, Frascati, Italy
[81] Physikalisches Institut, Albert-Ludwigs-Universität Freiburg, Freiburg, Germany
[82] II. Physikalisches Institut, Georg-August-Universität Göttingen, Göttingen, Germany
[83] Département de Physique Nucléaire et Corpusculaire, Université de Gen'eve, Gen'eve, Switzerland
[84] Dipartimento di Fisica, Università di Genova, Genova, Italy
[85] INFN Sezione di Genova, Italy
[86] II. Physikalisches Institut, Justus-Liebig-Universität Giessen, Giessen, Germany
[87] SUPA - School of Physics and Astronomy, University of Glasgow, Glasgow, United Kingdom
[88] LPSC, Université Grenoble Alpes, CNRS/IN2P3, Grenoble INP, Grenoble, France
[89] Laboratory for Particle Physics and Cosmology, Harvard University, Cambridge, MA, United States of America
[90] Department of Modern Physics and State Key Laboratory of Particle Detection and Electronics, University of Science and Technology of China, Hefei, China

[91] Kirchhoff-Institut für Physik, Ruprecht-Karls-Universität Heidelberg, Heidelberg, Germany
[92] Physikalisches Institut, Ruprecht-Karls-Universität Heidelberg, Heidelberg, Germany
[93] Department of Physics, Chinese University of Hong Kong, Shatin, N.T., Hong Kong, China
[94] Department of Physics, University of Hong Kong, Hong Kong, China
[95] Department of Physics, Institute for Advanced Study, Hong Kong University of Science and Technology, Clear Water Bay, Kowloon, Hong Kong, China
[96] Department of Physics, National Tsing Hua University, Hsinchu, Taiwan
[97] IJCLab, Université Paris-Saclay, CNRS/IN2P3, 91405, Orsay, France
[98] Centro Nacional de Microelectrónica (IMB-CNM-CSIC), Barcelona, Spain
[99] Department of Physics, Indiana University, Bloomington, IN, United States of America
[100] INFN Gruppo Collegato di Udine, Sezione di Trieste, Udine, Italy
[101] ICTP, Trieste, Italy
[102] Dipartimento Politecnico di Ingegneria e Architettura, Università di Udine, Udine, Italy
[103] INFN Sezione di Lecce, Italy
[104] Dipartimento di Matematica e Fisica, Università del Salento, Lecce, Italy
[105] INFN Sezione di Milano, Italy
[106] Dipartimento di Fisica, Università di Milano, Milano, Italy
[107] INFN Sezione di Napoli, Italy
[108] Dipartimento di Fisica, Università di Napoli, Napoli, Italy
[109] INFN Sezione di Pavia, Italy
[110] Dipartimento di Fisica, Università di Pavia, Pavia, Italy
[111] INFN Sezione di Pisa, Italy
[112] Dipartimento di Fisica E. Fermi, Università di Pisa, Pisa, Italy
[113] INFN Sezione di Roma, Italy
[114] Dipartimento di Fisica, Sapienza Università di Roma, Roma, Italy
[115] INFN Sezione di Roma Tor Vergata, Italy
[116] Dipartimento di Fisica, Università di Roma Tor Vergata, Roma, Italy
[117] INFN Sezione di Roma Tre, Italy
[118] Dipartimento di Matematica e Fisica, Università Roma Tre, Roma, Italy
[119] INFN-TIFPA, Italy
[120] Università degli Studi di Trento, Trento, Italy
[121] Department of Astro and Particle Physics, Universität Innsbruck, Innsbruck, Austria
[122] University of Iowa, Iowa City, IA, United States of America
[123] Department of Physics and Astronomy, Iowa State University, Ames, IA, United States of America
[124] Istinye University, Sariyer Istanbul, Türkiye
[125] Departamento de Engenharia Elétrica, Universidade Federal de Juiz de Fora (UFJF), Juiz de Fora, Brazil
[126] COPPE/EE/IF, Universidade Federal do Rio, De Janeiro Rio de Janeiro, Brazil
[127] Instituto de Física, Universidade de São Paulo, São Paulo, Brazil
[128] Janeiro State University, Rio de Janeiro, Brazil
[129] Federal University of Bahia, Bahia, Brazil
[130] KEK, High Energy Accelerator Research Organization, Tsukuba, Japan
[131] Khalifa University of Science and Technology, Abu Dhabi ,United Arab Emirates
[132] University of Sharjah, Sharjah, United Arab Emirates
[133] Graduate School of Science, Kobe University, Kobe, Japan
[134] Faculty of Physics and Applied Computer Science, AGH University of Krakow, Krakow, Poland
[135] Marian Smoluchowski Institute of Physics, Jagiellonian University, Krakow, Poland
[136] Institute of Nuclear Physics, Polish Academy of Sciences, Krakow, Poland
[137] Faculty of Science, Kyoto University, Kyoto, Japan
[138] Research Center for Advanced Particle Physics, Department of Physics, Kyushu University, Fukuoka, Japan
[139] L2IT, Université de Toulouse, CNRS/IN2P3, UPS, Toulouse, France
[140] Instituto de Física La Plata, Universidad Nacional de La Plata and CONICET, La Plata, Argentina
[141] Physics Department, Lancaster University, Lancaster, United Kingdom
[142] Oliver Lodge Laboratory, University of Liverpool, Liverpool, United Kingdom
[143] Department of Experimental Particle Physics, Department of Physics, Jožef Stefan Institute, University of Ljubljana, Ljubljana, Slovenia
[144] Department of Physics and Astronomy, Queen Mary University of London, London, United Kingdom
[145] Department of Physics, Royal Holloway University of London, Egham, United Kingdom
[146] Department of Physics and Astronomy, University College London, London, United Kingdom
[147] Louisiana Tech University, Ruston, LA, United States of America
[148] Fysiska institutionen, Lunds universitet, Lund, Sweden
[149] Departamento de Física Teorica C-15 and CIAFF, Universidad Autónoma de Madrid, Madrid, Spain
[150] Institut für Physik, Universität Mainz, Mainz, Germany
[151] School of Physics and Astronomy, University of Manchester, Manchester, United Kingdom
[152] CPPM, Aix-Marseille Université, CNRS/IN2P3, Marseille, France
[153] Department of Physics, University of Massachusetts, Amherst, MA, United States of America
[154] Department of Physics, McGill University, Montreal, QC, Canada
[155] School of Physics, University of Melbourne, Victoria, Australia
[156] Department of Physics, University of Michigan, Ann Arbor, MI, United States of America
[157] Department of Physics and Astronomy, Michigan State University, East Lansing, MI, United States of America
[158] Group of Particle Physics, University of Montreal, Montreal, QC, Canada
[159] Fakultät für Physik, Ludwig-Maximilians-Universität München, München, Germany
[160] Max-Planck-Institut für Physik (Werner-Heisenberg-Institut), München, Germany
[161] Graduate School of Science and Kobayashi-Maskawa Institute, Nagoya University, Nagoya, Japan
[162] Department of Physics, Nanjing University, Nanjing, China
[163] School of Science, Shenzhen Campus of Sun Yat-sen University, China
[164] University of Chinese Academy of Science (UCAS), Beijing, China
[165] Department of Physics and Astronomy, University of New Mexico, Albuquerque, NM, United States of America
[166] Institute for Mathematics, Astrophysics and Particle Physics, Nikhef, Radboud University, Nijmegen, Netherlands
[167] Nikhef National Institute for Subatomic Physics and University of Amsterdam, Amsterdam, Netherlands
[168] Department of Physics, Northern Illinois University, DeKalb, IL, United States of America
[169] New York University Abu Dhabi, Abu Dhabi, United Arab Emirates
[170] United Arab Emirates University, Al Ain, United Arab Emirates
[171] Department of Physics, New York University, New York, NY, United States of America
[172] Ochanomizu University, Bunkyo-ku, Otsuka Tokyo, Japan
[173] Ohio State University, Columbus, OH, United States of America
[174] Department of Physics and Astronomy, Homer L. Dodge, University of Oklahoma, Norman, OK, United States of America
[175] Department of Physics, Oklahoma State University, Stillwater, OK, United States of America
[176] Joint Laboratory of Optics, Palacký University, Olomouc, Czech Republic

[177] Institute for Fundamental Science, University of Oregon, Eugene, OR, United States of America
[178] Graduate School of Science, University of Osaka, Osaka, Japan
[179] Department of Physics, University of Oslo, Oslo, Norway
[180] Department of Physics, Oxford University, Oxford, United Kingdom
[181] LPNHE, Sorbonne Université, Université Paris Cité, CNRS/IN2P3, Paris, France
[182] Department of Physics, University of Pennsylvania, Philadelphia, PA, United States of America
[183] Department of Physics and Astronomy, University of Pittsburgh, Pittsburgh, PA, United States of America
[184] Laboratório de Instrumentação e Física Experimental de Partículas - LIP, Lisboa, Portugal
[185] Departamento de Física, Faculdade de Ciências, Universidade de Lisboa, Lisboa, Portugal
[186] Departamento de Física, Universidade de Coimbra, Coimbra, Portugal
[187] Centro de Física Nuclear da Universidade de Lisboa, Lisboa, Portugal
[188] Departamento de Física, Escola de Ciências, Universidade do Minho, Braga, Portugal
[189] Departamento de Física Teórica y del Cosmos, Universidad de Granada, Granada, Spain, Portugal
[190] Departamento de Física, Instituto Superior Técnico, Universidade de Lisboa, Lisboa, Portugal
[191] Institute of Physics, Czech Academy of Sciences, Prague, Czech Republic
[192] Czech Technical University, Prague Prague, Czech Republic
[193] Faculty of Mathematics and Physics, Charles University, Prague, Czech Republic
[194] Particle Physics Department, Rutherford Appleton Laboratory Didcot, United Kingdom
[195] IRFU, CEA, Université Paris-Saclay, Gif-sur-Yvette, France
[196] Santa Cruz Institute for Particle Physics, University of California Santa Cruz, Santa Cruz, CA, United States of America
[197] Departamento de Física, Pontificia Universidad Católica de Chile, Santiago, Chile
[198] Millennium Institute for Subatomic physics at high energy frontier (SAPHIR), Santiago, Chile
[199] Departamento de Física, Instituto de Investigación Multidisciplinario en Ciencia y Tecnología, Universidad de La Serena, Chile
[200] Department of Physics, Universidad Andres Bello, Santiago, Chile
[201] Universidad San Sebastian, Recoleta, Chile
[202] Instituto de Alta Investigaci, Universidad de Tarapacá, Arica, Chile
[203] Departamento de Física, Universidad Técnica Federico Santa María, Valparaíso, Chile
[204] Department of Physics, Institute of Science, Tokyo, Japan
[205] Department of Physics, University of Washington, Seattle, WA, United States of America
[206] Institute of Frontier and Interdisciplinary Science and Key, Laboratory of Particle Physics and Particle Irradiation (MOE), Shandong University, Qingdao, China
[207] School of Physics, Zhengzhou University, China
[208] School of Physics and Astronomy, State Key Laboratory of Dark Matter Physics, Shanghai Jiao Tong University, Key Laboratory for Particle Astrophysics and Cosmology (MOE), SKLPPC, Shanghai, China
[209] State Key Laboratory of Dark Matter Physics, Tsung-Dao Lee Institute, Shanghai Jiao Tong University, Shanghai, China
[210] Department of Physics and Astronomy, University of Sheffield, Sheffield, United Kingdom
[211] Department of Physics, Shinshu University, Nagano, Japan
[212] Department Physik, Universität Siegen, Siegen, Germany
[213] Department of Physics, Simon Fraser University, Burnaby, BC, Canada
[214] SLAC National Accelerator Laboratory, Stanford, CA, United States of America
[215] Department of Physics, Royal Institute of Technology, Stockholm, Sweden
[216] Departments of Physics and Astronomy, Stony Brook University, Stony Brook, NY, United States of America
[217] Department of Physics and Astronomy, University of Sussex, Brighton, United Kingdom
[218] School of Physics, University of Sydney, Sydney, Australia
[219] Institute of Physics, Academia Sinica, Taipei, Taiwan
[220] E. Andronikashvili Institute of Physics, Iv. Javakhishvili Tbilisi State University, Tbilisi, Georgia
[221] High Energy Physics Institute, Tbilisi State University, Tbilisi, Georgia
[222] University of Georgia, Tbilisi, Georgia
[223] Department of Physics, Israel Institute of Technology, Technion Haifa, Israel
[224] Beverly Sackler School of Physics and Astronomy, Tel Aviv University, Tel Aviv, Israel
[225] Department of Physics, Aristotle University of Thessaloniki, Thessaloniki, Greece
[226] International Center for Elementary Particle Physics, Department of Physics, University of Tokyo, Tokyo, Japan
[227] Graduate School of Science and Technology, Tokyo Metropolitan University, Tokyo, Japan
[228] Department of Physics, University of Toronto, Toronto, ON, Canada
[229] TRIUMF, Vancouver, BC, Canada
[230] Department of Physics and Astronomy, York University, Toronto, ON, Canada
[231] Division of Physics and Tomonaga Center, Faculty of Pure and Applied Sciences, the History of the Universe, University of Tsukuba, Tsukuba, Japan
[232] Department of Physics and Astronomy, Tufts University, Medford, MA, United States of America
[233] Department of Physics and Astronomy, University of California Irvine, Irvine, CA, United States of America
[234] University of West Attica, Athens, Greece
[235] Department of Physics and Astronomy, University of Uppsala, Uppsala, Sweden
[236] Department of Physics, University of Illinois, Urbana, IL, United States of America
[237] Centro Mixto, Instituto de Física Corpuscular (IFIC), Universidad de Valencia - CSIC, Valencia, Spain
[238] Department of Physics, University of British Columbia, Vancouver, BC, Canada
[239] Department of Physics and Astronomy, University of Victoria, Victoria, BC, Canada
[240] Fakultät für Physik und Astronomie, Julius-Maximilians-Universität Würzburg, Würzburg, Germany
[241] Department of Physics, University of Warwick, Coventry, United Kingdom
[242] Waseda University, Tokyo, Japan
[243] Department of Particle Physics and Astrophysics, Weizmann Institute of Science, Rehovot, Israel
[244] Department of Physics, University of Wisconsin, Madison, WI, United States of America
[245] Fachgruppe Physik, Fakultät für Mathematik und Naturwissenschaften, Bergische Universität Wuppertal, Wuppertal, Germany
[246] Department of Physics, Yale University, New Haven, CT, United States of America
[247] Yerevan Physics Institute, Yerevan, Armenia
[248] Also at Affiliated with an institute formerly covered by a cooperation agreement with CERN
[249] Also at An-Najah National University, Nablus, Palestine
[250] Also at Borough of Manhattan Community College, University of New York, City, New York NY, United States of America
[251] Also at Center for Interdisciplinary Research and Innovation (CIRI-AUTH), Thessaloniki, Greece

[252] Also at Centre of Physics, Universities of Minho and Porto (CF-UM-UP), Portugal
[253] Also at CERN, Geneva, Switzerland
[254] Also at Département de Physique Nucléaire et Corpusculaire, Université de Gen'eve, Gen'eve, Switzerland
[255] Departament de Fisica, Universitat Autonoma de Barcelona, Barcelona, Spain
[256] Department of Financial and Management Engineering, University of the Aegean, Chios, Greece
[257] Department of Mathematical Sciences, University of South Africa, Johannesburg, South Africa
[258] Department of Physics, Bolu Abant Izzet Baysal University, Bolu, Türkiye
[259] Department of Physics, King's, College London London, United Kingdom
[260] Department of Physics, Stanford University, Stanford, CA, United States of America
[261] Department of Physics, Stellenbosch University, South Africa
[262] Department of Physics, University of Fribourg, Fribourg, Switzerland
[263] Department of Physics, University of Thessaly, Greece
[264] Department of Physics, Westmont College, Santa Barbara, United States of America
[265] Also at Faculty of Physics, Sofia University, 'St. Kliment Ohridski', Sofia, Bulgaria
[266] Also at Faculty of Physics, University of Bucharest, Romania
[267] Also at Hellenic Open University, Patras, Greece
[268] Henan University, China
[269] Imam Mohammad Ibn Saud Islamic University, Saudi Arabia
[270] Institucio Catalana de Recerca i Estudis Avancats, ICREA, Barcelona, Spain
[271] Also at Institut für Experimentalphysik, Universität Hamburg, Hamburg, Germany
[272] Also at Institute for Nuclear Research and Nuclear Energy (INRNE), Bulgarian Academy of Sciences, Sofia, Bulgaria
[273] Also at Institute of Applied Physics, Mohammed VI Polytechnic University, Ben Guerir, Morocco
[274] Also at Institute of Particle Physics (IPP), Canada
[275] Also at Institute of Physics and Technology, Mongolian Academy of Sciences, Ulaanbaatar, Mongolia
[276] Also at Institute of Physics, Azerbaijan Academy of Sciences, Baku, Azerbaijan
[277] Also at Institute of Theoretical Physics, Ilia State University, Tbilisi, Georgia
[278] Also at Millennium Institute for Subatomic physics at high energy frontier (SAPHIR), Santiago, Chile
[279] National Institute of Physics, University of The Philippines Diliman (Philippines), Philippines
[280] The Collaborative Innovation Center of Quantum Matter (CICQM), Beijing, China
[281] Also at TRIUMF, Vancouver, BC, Canada
[282] Also at Università di Napoli Parthenope, Napoli, Italy
[283] University of Chinese Academy of Sciences (UCAS), Beijing, China
[284] Department of Physics, University of Colorado Boulder, Colorado, United States of America
[285] University of Siena, Italy
[286] Also at Washington College, Chestertown, MD, United States of America
[287] Physics Department, Yeditepe University, Istanbul, Türkiye
[288] Deceased

References

[1] ATLAS Collaboration, Observation of a new particle in the search for the standard model Higgs boson with the ATLAS detector at the LHC, Phys. Lett. B 716 (2012) 1. arXiv:1207.7214, https://doi.org/10.1016/j.physletb.2012.08.020
[2] CMS Collaboration, Observation of a new boson at a mass of 125 GeV with the CMS experiment at the LHC, Phys. Lett. B 716 (2012) 30. arXiv:1207.7235, https://doi.org/10.1016/j.physletb.2012.08.021
[3] L. Evans, P. Bryant, LHC machine, JINST 3 (2008) S08001. https://doi.org/10.1088/1748-0221/3/08/S08001
[4] ATLAS Collaboration, A detailed map of Higgs boson interactions by the ATLAS experiment ten years after the discovery, Nature 607 (2022) 52–59. arXiv:2207.00092, https://doi.org/10.1038/s41586-022-04893-w
[5] CMS Collaboration, A portrait of the Higgs boson by the CMS experiment ten years after the discovery, Nature 607 (2022) 60–68. arXiv:2207.00043, https://doi.org/10.1038/s41586-022-04892-x
[6] ATLAS Collaboration, Study of the spin and parity of the Higgs boson in diboson decays with the ATLAS detector, Eur. Phys. J. C 75 (2015) 476. arXiv:1506.05669, https://doi.org/10.1140/epjc/s10052-015-3685-1
[7] CMS Collaboration, Constraints on the spin-parity and anomalous HVV couplings of the Higgs boson in proton collisions at 7 and 8 TeV, Phys. Rev. D 92 (2015) 012004. arXiv:1411.3441, https://doi.org/10.1103/PhysRevD.92.012004
[8] C. ATLAS and Collaborations, Combined measurement of the Higgs boson mass in pp collisions at $\sqrt{s} = 7$ and 8 TeV with the ATLAS and CMS experiments, Phys. Rev. Lett. 114 (2015) 191803. arXiv:1503.07589, https://doi.org/10.1103/PhysRevLett.114.191803
[9] ATLAS Collaboration, Combined measurement of the Higgs boson mass from the $H \to \gamma\gamma$ and $H \to ZZ^* \to 4\ell$ decay channels with the ATLAS detector using $\sqrt{s} = 7, 8$, and 13 TeV pp collision data, Phys. Rev. Lett. 131 (2023) 251802. arXiv:2308.04775, https://doi.org/10.1103/PhysRevLett.131.251802
[10] CMS Collaboration, Measurement of the Higgs boson mass and width using the four-lepton final state in proton–proton collisions at $\sqrt{s} = 13$ TeV, Phys. Rev. D 111 (2024) 092014. arXiv:2409.13663, https://doi.org/10.1103/PhysRevD.111.092014
[11] CMS Collaboration, A measurement of the Higgs boson mass in the diphoton decay channel, Phys. Lett. B 805 (2020) 135425. arXiv:2002.06398, https://doi.org/10.1016/j.physletb.2020.135425
[12] D. de Florian, et al., LHC Higgs Cross Section Working Group, Handbook of LHC Higgs cross sections: 4. deciphering the nature of the Higgs sector (2017). arXiv:1610.07922, https://doi.org/10.23731/CYRM-2017-002
[13] M. Carena, I. Low, C.E.M. Wagner, Implications of a modified Higgs to diphoton decay width, JHEP 08 (2012) 060. arXiv:1206.1082, https://doi.org/10.1007/JHEP08(2012)060
[14] C.-W. Chiang, K. Yagyu, Higgs boson decays to $\gamma\gamma$ and $Z\gamma$ in models with Higgs extensions, Phys. Rev. D 87 (2013) 033003. arXiv:1207.1065, https://doi.org/10.1103/PhysRevD.87.033003
[15] C.-S. Chen, C.-Q. Geng, D. Huang, L.-H. Tsai, New scalar contributions to $h \to Z\gamma$, Phys. Rev. D 87 (2013) 075019. arXiv:1301.4694, https://doi.org/10.1103/PhysRevD.87.075019
[16] A. Djouadi, V. Driesen, W. Hollik, A. Kraft, The Higgs-photon-Z boson coupling revisited, Eur. Phys. J. C 1 (1-2) (1998) 163-175. arXiv:hep-ph/9701342, https://doi.org/10.1007/bf01245806
[17] H.T. Hung, T.T. Hong, H.H. Phuong, H.L.T. Mai, L.T. Hue, Neutral Higgs boson decays $H \to Z\gamma, \gamma\gamma$ in 3-3-1 models, Phys. Rev. D 100 (2019) 075014. arXiv:1907.06735, https://doi.org/10.1103/PhysRevD.100.075014
[18] P. Archer-Smith, D. Stolarski, R. Vega-Morales, On new physics contributions to the Higgs decay to $Z\gamma$, JHEP 2021 (10) (2021). arXiv:2012.01440, https://doi.org/10.1007/jhep10(2021)247
[19] X.-G. He, Z.-L. Huang, M.-W. Li, C.-W. Liu, The SM expected branching ratio for h $\to \gamma\gamma$ and an excess for h $\to$ Zγ, JHEP 10 (2024) 135. arXiv:2402.08190, https://doi.org/10.1007/JHEP10(2024)135
[20] A. Azatov, R. Contino, A. Di Iura, J. Galloway, New prospects for Higgs compositeness in $h \to Z\gamma$, Phys. Rev. D 88 (2013) 075019. arXiv:1308.2676, https://doi.org/10.1103/PhysRevD.88.075019
[21] I. Low, J. Lykken, G. Shaughnessy, Singlet scalars as Higgs boson imposters at the large hadron collider, Phys. Rev. D 84 (2011) 035027. arXiv:1105.4587, https://doi.org/10.1103/PhysRevD.84.035027
[22] I. Low, J. Lykken, G. Shaughnessy, Have we observed the Higgs boson (imposter)?, Phys. Rev. D 86 (2012) 093012. arXiv:1207.1093, https://doi.org/10.1103/PhysRevD.86.093012
[23] ATLAS Collaboration, A search for the $Z\gamma$ decay mode of the Higgs boson in pp collisions at $\sqrt{s} = 13$ TeV with the ATLAS detector, Phys. Lett. B 809 (2020) 135754. arXiv:2005.05382, https://doi.org/10.1016/j.physletb.2020.135754
[24] CMS Collaboration, Search for Higgs boson decays to a Z boson and a photon in proton–proton collisions at $\sqrt{s} = 13$ TeV, JHEP 05 (2023) 233. arXiv:2204.12945, https://doi.org/10.1007/JHEP05(2023)233
[25] C. Collaboration, ATLAS and Collaboration, Evidence for the Higgs boson decay to a Z boson and a photon at the LHC, Phys. Rev. Lett. 132 (2024) 021803. arXiv:2309.03501, https://doi.org/10.1103/PhysRevLett.132.021803
[26] T. Chen, C. Guestrin, XGBoost: a scalable tree boosting system, in: Proceedings of the 22nd ACM SIGKDD International Conference on Knowledge Discovery and Data Mining, ACM, 2016, pp. 785–794. arXiv:1603.02754, https://doi.org/10.1145/2939672.2939785
[27] ATLAS Collaboration, The ATLAS experiment at the CERN large hadron collider, JINST 3 (2008) S08003. https://doi.org/10.1088/1748-0221/3/08/S08003
[28] ATLAS Collaboration, The ATLAS experiment at the CERN large hadron collider: a description of the detector configuration for run 3, JINST 19 (2024) P05063. arXiv:2305.16623, https://doi.org/10.1088/1748-0221/19/05/P05063
[29] ATLAS Collaboration, Performance of the ATLAS trigger system in 2015, Eur. Phys. J. C 77 (2017) 317. arXiv:1611.09661, https://doi.org/10.1140/epjc/s10052-017-4852-3

[30] ATLAS Collaboration, The ATLAS trigger system for LHC run 3 and trigger performance in 2022, JINST 19 (2024) P06029. arXiv:2401.06630, https://doi.org/10.1088/1748-0221/19/06/P06029

[31] ATLAS Collaboration, Software and computing for run 3 of the ATLAS experiment at the LHC, Eur. Phys. J. C 85 (2025) 234. arXiv:2404.06335, https://doi.org/10.1140/epjc/s10052-024-13701-w

[32] ATLAS Collaboration, Performance of electron and photon triggers in ATLAS during LHC run 2, Eur. Phys. J. C 80 (2020) 47. arXiv:1909.00761, https://doi.org/10.1140/epjc/s10052-019-7500-2

[33] ATLAS Collaboration, Performance of the ATLAS muon triggers in run 2, JINST 15 (2020) P09015. arXiv:2004.13447, https://doi.org/10.1088/1748-0221/15/09/p09015

[34] S. Agostinelli, et al., GEANT4, Geant4-a simulation toolkit, Nucl. Instrum. Meth. A 506 (2003) 250. https://doi.org/10.1016/S0168-9002(03)01368-8

[35] ATLAS Collaboration, The ATLAS simulation infrastructure, Eur. Phys. J. C 70 (2010) 823. arXiv:1005.4568, https://doi.org/10.1140/epjc/s10052-010-1429-9

[36] C. Anastasiou, C. Duhr, F. Dulat, F. Herzog, B. Mistlberger, Higgs boson gluon-fusion production in QCD at three loops, Phys. Rev. Lett. 114 (2015) 212001. arXiv:1503.06056, https://doi.org/10.1103/PhysRevLett.114.212001

[37] C. Anastasiou, C. Duhr, F. Dulat, E. Furlan, T. Gehrmann, F. Herzog, A. Lazopoulos, B. Mistlberger, High precision determination of the gluon fusion Higgs boson cross-section at the LHC, JHEP 05 (2016) 058. arXiv:1602.00695, https://doi.org/10.1007/JHEP05(2016)058

[38] F. Dulat, A. Lazopoulos, B. Mistlberger, iHixs 2 – inclusive Higgs cross sections, Comput. Phys. Commun. 233 (2018) 243–260. arXiv:1802.00827, https://doi.org/10.1016/j.cpc.2018.06.025

[39] R.V. Harlander, K.J. Ozeren, Finite top mass effects for hadronic Higgs production at next-to-next-to-leading order, JHEP 11 (2009) 088. arXiv:0909.3420, https://doi.org/10.1088/1126-6708/2009/11/088

[40] R.V. Harlander, K.J. Ozeren, Top mass effects in Higgs production at next-to-next-to-leading order QCD: virtual corrections, Phys. Lett. B 679 (2009) 467–472. arXiv:0907.2997, https://doi.org/10.1016/j.physletb.2009.08.012

[41] R.V. Harlander, H. Mantler, S. Marzani, K.J. Ozeren, Higgs production in gluon fusion at next-to-next-to-leading order QCD for finite top mass, Eur. Phys. J. C 66 (2010) 359–372. arXiv:0912.2104, https://doi.org/10.1140/epjc/s10052-010-1258-x

[42] A. Pak, M. Rogal, M. Steinhauser, Finite top quark mass effects in NNLO Higgs boson production at LHC, JHEP 02 (2010) 025. arXiv:0911.4662, https://doi.org/10.1007/JHEP02(2010)025

[43] S. Actis, G. Passarino, C. Sturm, S. Uccirati, NLO electroweak corrections to Higgs boson production at hadron colliders, Phys. Lett. B 670 (2008) 12–17. arXiv:0809.1301, https://doi.org/10.1016/j.physletb.2008.10.018

[44] S. Actis, G. Passarino, C. Sturm, S. Uccirati, NNLO computational techniques: the cases $H \to \gamma\gamma$ and $H \to gg$, Nucl. Phys. B 811 (2009) 182–273. arXiv:0809.3667, https://doi.org/10.1016/j.nuclphysb.2008.11.024

[45] C. Anastasiou, R. Boughezal, F. Petriello, Mixed QCD-electroweak corrections to Higgs boson production in gluon fusion, JHEP 04 (2009) 003. arXiv:0811.3458, https://doi.org/10.1088/1126-6708/2009/04/003

[46] U. Aglietti, R. Bonciani, G. Degrassi, A. Vicini, Two-loop light fermion contribution to Higgs production and decays, Phys. Lett. B 595 (2004) 432–441. arXiv:hep-ph/0404071, https://doi.org/10.1016/j.physletb.2004.06.063

[47] M. Bonetti, K. Melnikov, L. Tancredi, Higher order corrections to mixed QCD-EW contributions to Higgs boson production in gluon fusion, Phys. Rev. D 97 (5) (2018) 056017. arXiv:1801.10403, https://doi.org/10.1103/PhysRevD.97.056017

[48] M. Ciccolini, A. Denner, S. Dittmaier, Strong and electroweak corrections to the production of a Higgs boson + 2Jets via weak interactions at the large hadron collider, Phys. Rev. Lett. 99 (2007) 161803. arXiv:0707.0381, https://doi.org/10.1103/PhysRevLett.99.161803

[49] M. Ciccolini, A. Denner, S. Dittmaier, Electroweak and QCD corrections to Higgs production via vector-boson fusion at the CERN LHC, Phys. Rev. D 77 (2008) 013002. arXiv:0710.4749, https://doi.org/10.1103/PhysRevD.77.013002

[50] P. Bolzoni, F. Maltoni, S.-O. Moch, M. Zaro, Higgs boson production via vector-boson fusion at next-to-next-to-leading order in QCD, Phys. Rev. Lett. 105 (2010) 011801. arXiv:1003.4451, https://doi.org/10.1103/PhysRevLett.105.011801

[51] M.L. Ciccolini, S. Dittmaier, M. Krämer, Electroweak radiative corrections to associated WH and ZH production at hadron colliders, Phys. Rev. D 68 (2003) 073003. arXiv:hep-ph/0306234, https://doi.org/10.1103/PhysRevD.68.073003

[52] O. Brein, A. Djouadi, R. Harlander, NNLO QCD corrections to the Higgs-strahlung processes at hadron colliders, Phys. Lett. B 579 (2004) 149–156. arXiv:hep-ph/0307206, https://doi.org/10.1016/j.physletb.2003.10.112

[53] O. Brein, R.V. Harlander, M. Wiesemann, T. Zirke, Top-quark mediated effects in hadronic Higgs-Strahlung, Eur. Phys. J. C 72 (2012) 1868. arXiv:1111.0761, https://doi.org/10.1140/epjc/s10052-012-1868-6

[54] L. Altenkamp, S. Dittmaier, R.V. Harlander, H. Rzehak, T.J.E. Zirke, Gluon-induced Higgs-Strahlung at next-to-leading order QCD, JHEP 02 (2013) 078. arXiv:1211.5015, https://doi.org/10.1007/JHEP02(2013)078

[55] A. Denner, S. Dittmaier, S. Kallweit, A. Mück, HAWK 2.0: a Monte Carlo program for Higgs production in vector-boson fusion and Higgs Strahlung at hadron colliders, Comput. Phys. Commun. 195 (2015) 161–171. arXiv:1412.5390, https://doi.org/10.1016/j.cpc.2015.04.021

[56] O. Brein, R.V. Harlander, T.J.E. Zirke, vh@nnlo-Higgs Strahlung at hadron colliders, Comput. Phys. Commun. 184 (2013) 998–1003. arXiv:1210.5347, https://doi.org/10.1016/j.cpc.2012.11.002

[57] R.V. Harlander, A. Kulesza, V. Theeuwes, T. Zirke, Soft gluon resummation for gluon-induced Higgs Strahlung, JHEP 11 (2014) 082. arXiv:1410.0217, https://doi.org/10.1007/JHEP11(2014)082

[58] R.V. Harlander, J. Klappert, S. Liebler, L. Simon, vh@nnlo-v2: new physics in Higgs Strahlung, JHEP 05 (2018) 089. arXiv:1802.04817, https://doi.org/10.1007/JHEP05(2018)089

[59] W. Beenakker, S. Dittmaier, M. Kramer, B. Plumper, M. Spira, P.M. Zerwas, NLO QCD corrections to $t\bar{t}H$ production in hadron collisions, Nucl. Phys. B 653 (2003) 151–203. arXiv:hep-ph/0211352, https://doi.org/10.1016/S0550-3213(03)00044-0

[60] S. Dawson, C. Jackson, L.H. Orr, L. Reina, D. Wackeroth, Associated Higgs boson production with top quarks at the CERN large hadron collider: NLO QCD corrections, Phys. Rev. D 68 (2003) 034022. arXiv:hep-ph/0305087, https://doi.org/10.1103/PhysRevD.68.034022

[61] Y. Zhang, W.-G. Ma, R.-Y. Zhang, C. Chen, L. Guo, QCD NLO and EW NLO corrections to $t\bar{t}H$ production with top quark decays at hadron collider, Phys. Lett. B 738 (2014) 1–5. arXiv:1407.1110, https://doi.org/10.1016/j.physletb.2014.09.022

[62] S. Frixione, V. Hirschi, D. Pagani, H.-S. Shao, M. Zaro, Electroweak and QCD corrections to top-pair hadroproduction in association with heavy bosons, JHEP 06 (2015) 184. arXiv:1504.03446, https://doi.org/10.1007/JHEP06(2015)184

[63] M. Wiesemann, R. Frederix, S. Frixione, V. Hirschi, F. Maltoni, P. Torrielli, Higgs production in association with bottom quarks, JHEP (2) (2015) 132. arXiv:1409.5301, https://doi.org/10.1007/jhep02(2015)132

[64] S. Dittmaier, M. Krämer, M. Spira, Higgs radiation off bottom quarks at the Fermilab tevatron and the CERN LHC, Phys. Rev. D 70 (7) (2004) 074010. arXiv:hep-ph/0309204, https://doi.org/10.1103/physrevd.70.074010

[65] S. Dawson, C.B. Jackson, L. Reina, D. Wackeroth, Exclusive Higgs boson production with bottom quarks at hadron colliders, Phys. Rev. D 69 (7) (2004) 074027. arXiv:hep-ph/0311067, https://doi.org/10.1103/physrevd.69.074027

[66] P. Nason, C. Oleari, NLO Higgs boson production via vector-boson fusion matched with shower in POWHEG, JHEP 02 (2010) 037. arXiv:0911.5299, https://doi.org/10.1007/JHEP02(2010)037

[67] S. Alioli, P. Nason, C. Oleari, E. Re, A general framework for implementing NLO calculations in shower Monte Carlo programs: the POWHEG BOX, JHEP 06 (2010) 043. arXiv:1002.2581, https://doi.org/10.1007/JHEP06(2010)043

[68] P. Nason, A new method for combining NLO QCD with shower Monte Carlo algorithms, JHEP 11 (2004) 040. arXiv:hep-ph/0409146, https://doi.org/10.1088/1126-6708/2004/11/040

[69] S. Frixione, P. Nason, C. Oleari, Matching NLO QCD computations with parton shower simulations: the POWHEG method, JHEP 11 (2007) 070. arXiv:0709.2092, https://doi.org/10.1088/1126-6708/2007/11/070

[70] H.B. Hartanto, B. Jäger, L. Reina, D. Wackeroth, Higgs boson production in association with top quarks in the POWHEG BOX, Phys. Rev. D 91 (9) (2015) 094003. arXiv:1501.04498, https://doi.org/10.1103/PhysRevD.91.094003

[71] R.D. Ball, et al., The PDF4LHC21 combination of global PDF fits for the LHC run III, J. Phys. G 49 (2022) 080501. arXiv:2203.05506, https://doi.org/10.1088/1361-6471/ac7216

[72] C. Bierlich, S. Chakraborty, N. Desai, L. Gellersen, I. Helenius, P. Ilten, L. Lönnblad, S. Mrenna, S. Prestel, C.T. Preuss, T. Sjöstrand, P. Skands, M. Utheim, R. Verheyen, A comprehensive guide to the physics and usage of PYTHIA 8.3, SciPost Phys. Codeb. (2022) 8. arXiv:2203.11601, https://doi.org/10.21468/SciPostPhysCodeb.8

[73] L.-B. Chen, C.-F. Qiao, R.L. Zhu, Reconstructing the 125 GeV SM Higgs boson through $\ell\bar{\ell}\gamma$, Phys. Lett. B 726 (1) (2013) 306–311. arXiv:1211.6058, https://doi.org/10.1016/j.physletb.2013.08.050

[74] J. Bellm, G. Bewick, S. Ferrario Ravasio, S. Gieseke, D. Grellscheid, P. Kirchgaeßer, F. Loshaj, M.R. Masouminia, G. Nail, A. Papaefstathiou, S. Plätzer, R. Podskubka, M. Rauch, C. Reuschle, P. Richardson, P. Schichtel, M.H. Seymour, A. Siódmok, S. Webster, Herwig 7.2 release note, Eur. Phys. J. C 80 (5) (2020). arXiv:1912.06509, https://doi.org/10.1140/epjc/s10052-020-8011-x

[75] E. Bothmann, et al., Event generation with Sherpa 2.2, SciPost Phys. 7 (3) (2019) 034. arXiv:1905.09127, https://doi.org/10.21468/SciPostPhys.7.3.034

[76] NNPDF Collaboration, R.D. Ball, et al., Parton distributions for the LHC run II, JHEP 04 (2015) 040. arXiv:1410.8849, https://doi.org/10.1007/JHEP04(2015)040

[77] ATLAS Collaboration, AtlFast3: the next generation of fast simulation in ATLAS, Comput. Softw. Big Sci. 6 (2022) 7. arXiv:2109.02551, https://doi.org/10.1007/s41781-021-00079-7

[78] J. Alwall, R. Frederix, S. Frixione, V. Hirschi, F. Maltoni, O. Mattelaer, H.-S. Shao, T. Stelzer, P. Torrielli, M. Zaro, The automated computation of tree-level and next-to-leading order differential cross sections, and their matching to parton shower simulations, JHEP 07 (2014) 079. arXiv:1405.0301, https://doi.org/10.1007/JHEP07(2014)079

[79] R.D. Ball, V. Bertone, S. Carrazza, L. Del Debbio, S. Forte, A. Guffanti, N.P. Hartland, J. Rojo, Parton distributions with QED corrections, Nucl. Phys. B 877 (2) (2013) 290–320. arXiv:1308.0598, https://doi.org/10.1016/j.nuclphysb.2013.10.010

[80] ATLAS Collaboration, ATLAS Pythia 8 tunes to 7 TeV data, ATL-PHYS-PUB-2014-021, 2014. https://cds.cern.ch/record/1966419.

[81] K. Werner, F.-M. Liu, T. Pierog, Parton ladder splitting and the rapidity dependence of transverse momentum spectra in deuteron–gold collisions at the BNL relativistic heavy ion collider, Phys. Rev. C 74 (2006) 044902. arXiv:hep-ph/0506232, https://doi.org/10.1103/PhysRevC.74.044902

[82] T. Pierog, I. Karpenko, J.M. Katzy, E. Yatsenko, K. Werner, EPOS LHC: test of collective hadronization with data measured at the CERN large hadron collider, Phys. Rev. C 92 (2015) 034906. arXiv:1306.0121, https://doi.org/10.1103/PhysRevC.92.034906

[83] ATLAS Collaboration, The Pythia 8 A3 tune description of ATLAS minimum bias and inelastic measurements incorporating the Donnachie–Landshoff diffractive model, ATL-PHYS-PUB-2016-017, 2016. https://cds.cern.ch/record/2206965.

[84] G. Luisoni, P. Nason, C. Oleari, F. Tramontano, $HW^{\pm}$/HZ + 0 and 1 jet at NLO with the POWHEG BOX interfaced to GoSam and their merging within MiNLO, JHEP 10 (2013) 083. arXiv:1306.2542, https://doi.org/10.1007/JHEP10(2013)083

[85] L. Altenkamp, S. Dittmaier, R.V. Harlander, H. Rzehak, T.J.E. Zirke, Gluon-induced Higgs-strahlung at next-to-leading order QCD, JHEP 2013 (2) (2013) 78. arXiv:1211.5015, https://doi.org/10.1007/jhep02(2013)078

[86] R.V. Harlander, A. Kulesza, V. Theeuwes, T. Zirke, Soft gluon resummation for gluon-induced Higgs Strahlung, JHEP 2014 (11) (2014) 82. arXiv:1410.0217, https://doi.org/10.1007/jhep11(2014)082

[87] H.B. Hartanto, B. Jäger, L. Reina, D. Wackeroth, Higgs boson production in association with top quarks in the POWHEG BOX, Phys. Rev. D 91 (9) (2015) 094003. arXiv:1501.04498, https://doi.org/10.1103/physrevd.91.094003

[88] B. Jäger, L. Reina, D. Wackeroth, Higgs boson production in association with b jets in the POWHEG BOX, Phys. Rev. D 93 (1) (2016) 014030. arXiv:1509.05843, https://doi.org/10.1103/PhysRevD.93.014030

[89] ATLAS Collaboration, Vertex Reconstruction Performance of the ATLAS Detector at $\sqrt{s} = 13$ TeV, ATL-PHYS-PUB-2015-026, 2015. https://cds.cern.ch/record/2037717.

[90] ATLAS Collaboration, Muon reconstruction and identification efficiency in ATLAS using the full run 2 pp collision data set at $\sqrt{s} = 13$ TeV, Eur. Phys. J. C 81 (2021) 578. arXiv:2012.00578, https://doi.org/10.1140/epjc/s10052-021-09233-2

[91] ATLAS Collaboration, Studies of the muon momentum calibration and performance of the ATLAS detector with pp collisions at $\sqrt{s} = 13$ TeV, Eur. Phys. J. C 83 (2023) 686. arXiv:2212.07338, https://doi.org/10.1140/epjc/s10052-023-11584-x

[92] ATLAS Collaboration, Electron and photon performance measurements with the ATLAS detector using the 2015–2017 LHC proton–proton collision data, JINST 14 (2019) P12006. arXiv:1908.00005, https://doi.org/10.1088/1748-0221/14/12/P12006

[93] ATLAS Collaboration, Electron and photon efficiencies in LHC run 2 with the ATLAS experiment, JHEP 05 (2024) 162. arXiv:2308.13362, https://doi.org/10.1007/JHEP05(2024)162

[94] ATLAS Collaboration, Electron and photon energy calibration with the ATLAS detector using LHC run 2 data, JINST 19 (2024) P02009. arXiv:2309.05471, https://doi.org/10.1088/1748-0221/19/02/P02009

[95] ATLAS Collaboration, Jet reconstruction and performance using particle flow with the ATLAS detector, Eur. Phys. J. C 77 (2017) 466. arXiv:1703.10485, https://doi.org/10.1140/epjc/s10052-017-5031-2

[96] M. Cacciari, G.P. Salam, G. Soyez, The anti-k_t jet clustering algorithm, JHEP 04 (2008) 063. arXiv:0802.1189, https://doi.org/10.1088/1126-6708/2008/04/063

[97] M. Cacciari, G.P. Salam, G. Soyez, FastJet user manual, Eur. Phys. J. C 72 (2012) 1896. arXiv:1111.6097, https://doi.org/10.1140/epjc/s10052-012-1896-2

[98] ATLAS Collaboration, Jet energy scale and resolution measured in proton–proton collisions at $\sqrt{s} = 13$ TeV with the ATLAS detector, Eur. Phys. J. C 81 (2021) 689. arXiv:2007.02645, https://doi.org/10.1140/epjc/s10052-021-09402-3

[99] ATLAS Collaboration, Performance of pile-up mitigation techniques for jets in pp collisions at $\sqrt{s} = 8$ TeV using the ATLAS detector, Eur. Phys. J. C 76 (2016) 581. arXiv:1510.03823, https://doi.org/10.1140/epjc/s10052-016-4395-z

[100] ATLAS Collaboration, Forward jet vertex tagging using the particle flow algorithm, ATL-PHYS-PUB-2019-026, 2019. https://cds.cern.ch/record/2683100.

[101] Particle Data Group, Review of particle physics, PTEP 2020 (8) (2020) 083C01. https://doi.org/10.1093/ptep/ptaa104

[102] OPAL Collaboration, Search for anomalous production of di-lepton events with missing transverse momentum in e^+e^- collisions at $\sqrt{s} = 161$ and 172 GeV, Eur. Phys. J. C 4 (1) (1998) 47–74. arXiv:hep-ex/9710010, https://doi.org/10.1007/pl00021655

[103] M. Vesterinen, T.R. Wyatt, A novel technique for studying the Z boson transverse momentum distribution at hadron colliders, Nucl. Instrum. Meth. A 602 (2) (2009) 432–437. arXiv:0807.4956, https://doi.org/10.1016/j.nima.2009.01.203

[104] D. Rainwater, R. Szalapski, D. Zeppenfeld, Probing color-singlet exchange in Z + 2-jet events at the CERN LHC, Phys. Rev. D 54 (1996) 6680–6689. arXiv:hep-ph/9605444, https://doi.org/10.1103/PhysRevD.54.6680

[105] ATLAS Collaboration, ATLAS, Search for scalar diphoton resonances in the mass range 65–600 GeV with the ATLAS detector in pp collision data at $\sqrt{s} = 8\ TeV$, Phys. Rev. Lett. 113 (17) (2014) 171801. arXiv:1407.6583, https://doi.org/10.1103/PhysRevLett.113.171801

[106] ATLAS Collaboration, Measurement of the inclusive isolated prompt photon cross section in pp collisions at $\sqrt{s} = 7$ TeV with the ATLAS detector, Phys. Rev. D 83 (2011) 052005. arXiv:1012.4389, https://doi.org/10.1103/PhysRevD.83.052005

[107] A. Wald, Sequential tests of statistical hypotheses, Ann. Math. Statist. 16 (2) (1945) 117 – 186. arXiv:1007.4278, https://doi.org/10.1214/aoms/1177731118

[108] ATLAS Collaboration, Measurement of the properties of Higgs boson production at $\sqrt{s} = 13$ TeV in the $H \to \gamma\gamma$ channel using 139 fb^{-1} of pp collision data with the ATLAS experiment, JHEP 07 (2023) 088. arXiv:2207.00348, https://doi.org/10.1007/JHEP07(2023)088

[109] M. Frate, K. Cranmer, S. Kalia, A. Vandenberg-Rodes, D. Whiteson, Modeling smooth backgrounds and generic localized signals with Gaussian processes, 2017. arXiv:1709.05681

[110] ATLAS Collaboration, A search for the dimuon decay of the standard model Higgs boson with the ATLAS detector, Phys. Lett. B 812 (2021) 135980. arXiv:2007.07830, https://doi.org/10.1016/j.physletb.2020.135980

[111] G. Avoni, et al., The new LUCID-2 detector for luminosity measurement and monitoring in ATLAS, JINST 13 (2018) P07017. https://doi.org/10.1088/1748-0221/13/07/P07017

[112] ATLAS Collaboration, Preliminary analysis of the luminosity calibration of the ATLAS 13.6 TeV data recorded in 2022, ATL-DAPR-PUB-2023-001, 2023. https://cds.cern.ch/record/2853525.

[113] ATLAS Collaboration, Preliminary analysis of the luminosity calibration for the ATLAS 13.6 TeV data recorded in 2023, ATL-DAPR-PUB-2024-001, 2024. https://cds.cern.ch/record/2900949.

[114] G. Cowan, K. Cranmer, E. Gross, O. Vitells, Asymptotic formulae for likelihood-based tests of new physics, Eur. Phys. J. C 71 (2011) 1554. arXiv:1007.1727, https://doi.org/10.1140/epjc/s10052-011-1554-0

[115] ATLAS Collaboration, Search for Higgs boson decays to a photon and a Z boson in pp collisions at $\sqrt{s} = 7$ and 8 TeV with the ATLAS detector, Phys. Lett. B 732 (2014) 8. arXiv:1402.3051, https://doi.org/10.1016/j.physletb.2014.03.015

[116] ATLAS Collaboration, ATLAS Computing Acknowledgements, ATL-SOFT-PUB-2025-001, 2025. https://cds.cern.ch/record/2922210.